Sea Anemones through X-rays: Visualization of Two Species of *Diadumene* (Cnidaria, Actiniaria) Using Micro-CT

LUCIANA C. GUSMÃO,[1] ALEJANDRO GRAJALES,[1,2]
AND ESTEFANIA RODRÍGUEZ[1]

ABSTRACT

Diadumenidae is a monogeneric family comprised of 10 valid species in the genus *Diadumene*. Although these species are distributed in all but the Southern Ocean, *Diadumene lineata* is a cosmopolitan species and one of the most widely distributed marine organisms. Recent phylogenetic analyses with multiple species have recovered Diadumenidae as a monophyletic group with high support. Although generic placement is straightforward, species-level identifications within *Diadumene* are difficult because species are defined by a mosaic of characters that vary in degree rather than kind. Two species of the genus have been recorded in the southwestern Atlantic: *D. paranaensis* along the south coast of Brazil and *D. lineata* along the southeast and northeast coasts of Brazil as well as in Argentina. Here we record *D. leucolena* for the first time in the southern hemisphere and describe *D. manezinha*, sp. nov., raising to four the number of species of *Diadumene* for Brazil and to 11 worldwide. We incorporated microcomputed tomography (micro-CT) into the description of both species in the first application of the method for Actiniaria. We evaluate the utility of micro-CT imaging and its potential to generate fast, low-cost, and high-resolution datasets despite the anemone's low-density soft tissue. We present a protocol for sample handling, chemical staining, and scanning parameters that resulted in satisfactory imaging of the two specimens examined. We also analyze advantages and limitations of using micro-CT over traditional techniques in the study of sea anemones.

[1] Department of Invertebrate Zoology, American Museum of Natural History, New York.
[2] Departamento de Ciencias Biológicas, Universidad de los Andes, Bogotá, Colombia.

INTRODUCTION

Members of the family Diadumenidae Stephenson, 1920, are characterized by monotypic mesenteries, two types of nematocysts in the acontia, cinclides on the scapus, absence of marginal sphincter musculature, and ephemeral fighting tentacles. This monogeneric family is comprised of 10 valid species belonging to the genus *Diadumene* Stephenson, 1920, which is distributed in all but the Southern Ocean, albeit most species are restricted to the Atlantic Ocean (Fautin, 2013). *Diadumene lineata* (Verrill, 1869a), however, is a cosmopolitan species and one of the most widely distributed marine organisms (Minasian, 1982). The species is believed to be native to Southeast Asia (Uchida, 1932; Stephenson, 1935) and exotic in many regions of the world (see Fautin, 2013), possibly transported between localities by rafting on floating material or on the hulls of ships (Shick and Lamb, 1977; Gollasch and Riemann-Zürneck, 1996; Zabin et al., 2004; Farrapeira et al., 2007, 2010).

Diadumenidae has been recovered as monophyletic and closely related to members of Metridiidae Carlgren, 1893, in all molecular phylogenetic analyses including multiple species of the genus (Daly et al., 2008; Rodríguez and Daly, 2010; Gusmão and Daly, 2010; Rodríguez et al., 2012, 2014; Grajales and Rodríguez, 2016). Rodríguez et al. (2012) erected the clade Metridina for members of Diadumenidae and Metridiidae, emphasizing the morphological similarities among these families, which had been proposed by others (e.g., Stephenson, 1925). Similarly, a monophyletic *Diadumene* has been recovered with high support in recent studies including multiple species of the genus (Rodríguez et al., 2012, 2014; Lauretta et al., 2014; Grajales and Rodríguez, 2016). Although generic placement is straightforward, species-level identifications within *Diadumene* are difficult because species are defined by a mosaic of characters that vary in degree rather than kind.

Two species of *Diadumene* have been recorded in the southwestern Atlantic: *Diadumene paranaensis* Beneti et al., 2015, has been collected only on the southern coast of Brazil and *D. lineata* collected in the southeast and northeast of Brazil (Belém and Monteiro, 1977; Zamponi et al., 1998; Farrapeira et al., 2007; Da Silveira and Morandini, 2011; Rocha et al., 2013) as well as in Argentina (Acuña et al., 2004; Excoffon et al., 2004, Molina et al., 2009). Here we record *Diadumene leucolena* (Verrill, 1866) for the first time in the southern hemisphere and describe *D. manezinha*, sp. nov., raising to four the number of *Diadumene* species recorded in Brazil and to 11 worldwide. In addition, we incorporate microcomputed tomography (micro-CT) to the description of both species examined in the first application of the method for soft-bodied members of order Actiniaria Hertwig, 1882. Micro-CT reconstructions have efficiently delineated morphological features in other cnidarians (scleractinians: e.g., Kruszynski et al., 2006, Roche et al., 2010, Sentoku et al., 2015; jellyfish and staurozoans: Holst et al., 2016; octocorals: Morales Pinzón et al., 2014; hydrozoans: Puce et al., 2011) as well as other small soft-bodied invertebrates with no chitinous or calcified tissues (e.g., leeches: Tessler et al., 2016; earthworms: Fernández et al., 2014). Here we evaluate the utility of micro-CT imaging and its potential to generate fast, low-cost, and high-resolution datasets, despite the need for chemical staining due to the sea anemone's low-density soft tissue (Faulwetter et al., 2013a, 2013b). We present a protocol for sample handling, chemical staining, and scanning parameters that resulted in satisfactory imaging of both specimens examined. We compare advantages and limitations of using micro-CT over traditional techniques used in the taxonomy of sea anemones.

MATERIAL AND METHODS

Morphological study: Specimens of *Diadumene leucolena* were collected by hand in the intertidal zone of Praia do Farol Velho (0°35′33″S; 47°19′29.00″W) and Praia do Atalaia (0°35′36″S; 47°18′44.00″W) both in Salinópolis (Pará) on the north coast of Brazil (fig. 1). Specimens of *D. manezinha*, sp. nov., were collected by hand in Praia da Barra da Lagoa (27°35′4.49″ S, 48°26′10.45″ W) in Florianópolis (Santa Catarina) on the south coast of Brazil (fig. 1). Animals were relaxed using menthol crystals, photographed alive, and subsequently fixed in 10% seawater-formalin. Before fixation, small pieces of column or pedal disc from selected specimens were fixed in absolute ethanol for DNA analysis. The material was deposited in the Museu de Zoologia da Universidade de São Paulo (MZUSP) as follows: 10 formalin-fixed specimens of *D. leucolena* (MZUSP 002482) and 10 corresponding ethanol-fixed vouchers (MZUSP 2472–2481), and 20 formalin-fixed specimens of *D. manezinha* (MZUSP 002504) and six corresponding ethanol-fixed vouchers (MZUSP 2498–2503).

Formalin-fixed specimens were examined whole, dissected, and as serial sections. Fragments of three specimens of each species were dehydrated and embedded in paraffin. Histological sections 8–10 µm thick were stained with Heidenhain's Azan Triple Stain (Presnell and Schreibman, 1997). Cnidae capsules were identified and measured in squash preparations of tissue from tentacles, column, actinopharynx, filaments, and acontia of preserved specimens. These preparations were examined using differential interference microscopy (DIC) at 1000× magnification and, except for the rarer types, at least 20 undischarged capsules were measured to generate range, mean, and standard deviation for each type of cnida. Although the mean and standard deviation calculated are not statistically significant, they are shown to give an idea of size distribution in the length and width of undischarged capsules. The presence of each type of cnida in each tissue was confirmed on histological slides. We follow a nematocyst terminology similar to the one used by Sanamyan et al. (2012), which combines the classification of Weill (1934), modified by Carlgren (1940) and thus differentiating "basitrichs" from "*b*-mastigophores," with that of Schmidt (1969, 1972, 1974), which captures the underlying variation seen in "rhabdoids." Unlike Sanamyan et al. (2012), we do not modify Schmidt's (1969, 1972, 1974) nomenclature with den Hartog's (1995) notes on *p*-mastigophores B1 (see Discussion), but agree with the use of "mastigophore" instead of "rhabdoid" to preserve stability. We use a combination of classifications to better capture the underlying variation in cnida morphology given its imperative nature to actiniarian taxonomy, but do not imply any evolutionary relationship among these types. We include photographs of each type of nematocyst for reliable comparison across terminologies and taxa (see Fautin, 1988). Higher-level classification for Actiniaria follows Rodríguez et al. (2014).

Molecular methodology: Genomic DNA was isolated from approximately 25 mg of tissue using the Qiagen DNeasy kit. Whole genomic DNA was amplified using published primers and protocol detailed in Lauretta et al. (2014) for the mitochondrial markers 12S and16S. Sequences for nuclear 18S were amplified using ribosomal genes (see Grajales and Rodríguez, 2016, for details on amplification protocol and sequencing with newly designed primers specific to Actiniaria to avoid co-amplification of *Symbiodinium* Freudenthal,

1962). PCR products were cleaned using ExosapIT (Exonuclease I and FastAP thermosensitive alkaline phosphatase per manufacturer's specifications, except that shrimp alkaline phosphatase was replaced with FastAP). Cycle-sequencing reactions used a total of 5 µL of cleaned PCR product, at a concentration of 25 ng of product for every 200 base pairs (bp) of marker length. Cycle-sequencing products were cleaned using Centri-Sept columns (Princeton Separations; following the manufacturer's protocol) containing DNA-grade Sephadex (G-50 fine; GE Healthcare) and later sequenced using PCR amplification primers on an ABI 3770x at the in-house facilities of the American Museum of Natural History (AMNH). Forward and reverse sequences were assembled and edited in Geneious v.11.1.4 (Kearse et al., 2012) and blasted against the nucleotide database of GenBank to confirm that the obtained sequences corresponded to the target sequence/organism and not to their endosymbiotic algae. Sequences have been deposited in GenBank (see Supplementary Data: https://doi.org/10.5531/sd.sp.33). DNA sequences for each of the three markers were combined and analyzed with sequences corresponding to superfamily Metridioidea Carlgren, 1893, from Rodríguez et al. (2014), using sequences from selected taxa within the superfamily Actinioidea Rafinesque, 1815, as outgroup. Sequences for each marker were separately aligned using MAFFT v.7.017 (Katoh et al., 2002) using the following settings: Strategy, E-INS-I; Scoring matrix for nucleotide sequences, 200PAM/k = 2; Gap open penalty, 1.53; Offset value, 0.05. Alignments for each marker were analyzed separately and as a concatenated dataset.

PHYLOGENETIC INFERENCE: For each gene region, the best model of nucleotide substitution was chosen using the software PartitionFinder v.1.1.1 (Lanfear et al., 2012). Maximum-likelihood (ML) analyses were performed using RAxML v.7.6.3 (Stamatakis, 2006) as implemented on the CIPRES portal (Miller et al., 2010), using a different partition per gene. The majority rule criterion implemented in RAxML (-autoMRE) was used to assess clade support. Analyses were run with gaps treated as missing data.

CT-SCAN METHODOLOGY: The staining protocols for micro-CT scan and image processing were modified from those of Tessler et al. (2016). Specimens fixed and preserved in 10% formalin since 2012, were transferred to seawater for 30 min and subsequently completely submerged in 0.2M cacodylate buffer. Samples were postfixed in 1% osmium tetroxide for 1.5 hr at room temperature. Due to the autolimiting nature of the osmium tetroxide, which prevents penetration, the mix of osmium-cacodylate buffer was injected into the gastrovascular cavity of the anemones using a microsyringe to ensure a homogeneous exposure to the stain. Samples were prepared for scanning by a series of washes; the first step consisted of 30 min in phosphate buffer, followed by a second step of 15 min in fresh phosphate buffer, and two washes of 100% ethanol for 30 and 15 min, respectively. Once stained and washed, samples were transferred to a 50 ml polyethylene tube filled with fresh 100% ethanol in which they were kept until scanning. Both specimens were scanned in the same tube with 100% ethanol on a phoenix v|tome|x s240 GE (General Electric, Fairfield, CT, USA) at 60 kV and 70 µA with a molybdenum target, for a resolution of 4.72 microns/voxel for *Diadumene leucolena* and 14.98 microns/voxel for *D. mane-*

zinha. The exposure time for the detector varied from 500.155 ms for *D. leucolena* to 1,500.263 ms for *D. manezinha*. Reconstruction of the raw data was done using the software Phoenix datos|x (General Electric, Wunstorf, Germany) and the resulting files and images were processed and edited using the software VGStudio Max 3.0 (Volume Graphics, Heidelberg, Germany). Full micro-CT scan data and volumetric renderings are deposited in the Morphobase (www.morphosource.org) under project MZUSP-IZ002504.

SOURCE OF MATERIAL: Specimens examined are retained in the following institutions: MNRJ, Museum Nacional/ Universidade do Rio de Janeiro; MZUSP, Museu de Zoologia da Universidade de São Paulo; YPM, Yale Peabody Museum; ZMUC, University of Copenhagen Zoological Museum.

RESULTS

Order Actiniaria Hertwig, 1882

Suborder Enthemonae Rodríguez and Daly, 2014, in Rodríguez et al., 2014

Superfamily Metridioidea Carlgren, 1893

Family Diadumenidae Stephenson, 1920

DIAGNOSIS (modified from Carlgren, 1949; modifications in bold, additions in italics): **Metridioidean** with acontia with basitrichs and *p*-mastigophores **B2a** *or basitrichs,* p-*mastigophores B1, and* p-*mastigophores B2a*. No distinct marginal sphincter. **Tentacles of first and sometimes second cycle** may form **fighting** tentacles with holotrichs; these tentacles are ephemeral and may be totally absent in some species or population of species that possess them.

REMARKS: We modified the familial diagnosis to reflect recent changes in higher-level classification of Actiniaria (i.e., Rodríguez et al., 2012, 2014) and the terminology used to classify nematocysts in this study (i.e., modified from Sanamayan et al., 2012). These modifications have been made in all other diagnoses included in this study. We have also changed the diagnosis to include having only basitrichs and *p*-mastigophores B2a in the acontia of most species within the family but also basitrichs, *p*-mastigophores B1, and *p*-mastigophores B2a seen in *Diadumene lineata,* the only species of the genus with three categories of nematocysts in the acontia. In addition, the term "catch tentacles" of Carlgren (1929: *Fangtentakeln*) has been replaced by "fighting tentacles" to better reflect their searching and intraspecific agonistic behavior rather than feeding (Purcell, 1977; Williams, 1975; Fukui, 1986; Häussermann, 2003; Kovtun et al., 2012). Although fighting tentacles are not present in all species of Diadumenidae and many have warned against using them as a taxonomic character (e.g., Riemann-Zürneck, 1975), we chose to keep the presence of this character in the diagnosis given its uniqueness within Actiniaria and its presence in the type species of the genus (i.e., *Diadumene schilleriana* Stoliczka, 1869). We also specified that tentacles of first but sometimes also second cycles may form fighting tentacles and emphasized that they

may be ephemeral even in species that possess them. The presence of atrichs in fighting tentacles included by Carlgren (1949) was modified to holotrichs as these nematocysts are now recognized as having small spines (Edmands and Fautin, 1991). We have modified the last sentence of the diagnosis to emphasize that fighting tentacles may be completely absent (or may never have been observed) in certain species (i.e., *Diadumene fransciscana* Hand, 1956, and *Diadume lighti* Hand, 1956) or may be ephemeral in an individual's lifespan on species that possess them (e.g., West Coast populations of *D. leucolena* from California: Hand, 1956).

INCLUDED GENERA: *Diadumene* Stephenson, 1920.

Genus *Diadumene* Stephenson, 1920

DIAGNOSIS (adapted from Carlgren, 1949, and Hand, 1956; modifications in bold and additions in italics): Diadumenidae with well-developed pedal disc. Column smooth, divisible into scapus and capitulum separated by a collar. Scapus with cinclides *scattered or arranged in longitudinal rows; sometimes on top of raised projections.* No distinct marginal sphincter. Margin of capitulum tentaculate. Tentacles long, smooth, numerous, retractile, regularly arranged *except if asexual reproduction is present.* **Tentacles of first and second cycles** may form **fighting tentacles**, typically thicker than feeding tentacles and containing holotrichs among other nematocysts; these may be absent in *some species or individuals of species that possess them.* Outer tentacles may have *p*-**mastigophores B2b.** Six pairs of perfect mesenteries, two siphonoglyphs, and two pairs of directives usually present; their number may vary due to asexual reproduction. Mesenteries more numerous distally than proximally. Retractors diffuse, more or less restricted. Parietobasilar and basilar musculatures weak. Perfect mesenteries and stronger imperfect ones fertile. Acontia with basitrichs and *p*-**mastigophores B2a** *or basitrichs, p-mastigophores B1, and p-mastigophores B2a.* Cnidom: spirocysts, basitrichs, *p*-mastigophores A, *p*-**mastigophores *B1*, *p*-mastigophores B2a**, *p*-**mastigophores B2b,** and holotrichs.

REMARKS: Similar modifications made for the familial diagnosis regarding changes on higher-level classification (i.e., Rodríguez et al., 2012, 2014) and nematocyst terminology (i.e., Sanamyan et al., 2012) were also made here. We have also included specific information on location of cinclides on the scapus (i.e., scattered or arranged in longitudinal rows) and position on top of raised columnar projections (e.g., *Diadumene leucolena*). The *p*-mastigophores B2b with looped basal tubule of outer tentacles were identified as macrobasic amastigophores in previous diagnoses of the genus (e.g., Stephenson, 1920; Carlgren, 1949; Hand, 1956). We have added the presence of *p*-mastigophores A to the diagnosis of the genus as this nematocyst has been found in *D. lineata* (Kovtun et al., 2012), *Diadumene neozelanica* Carlgren, 1924a, and *D. manezinha.*

TYPE SPECIES: *Sagartia schilleriana* Stoliczka, 1869, by monotypy.

INCLUDED SPECIES: *Diadumene cincta* Stephenson, 1925; *Diadumene crocata* (Hutton, 1880); *D. fransciscana; Diadumene kameruniensis* Carlgren, 1927; *D. leucolena; D. lighti; D. lineata; D. neozelanica; D. paranaensis.*
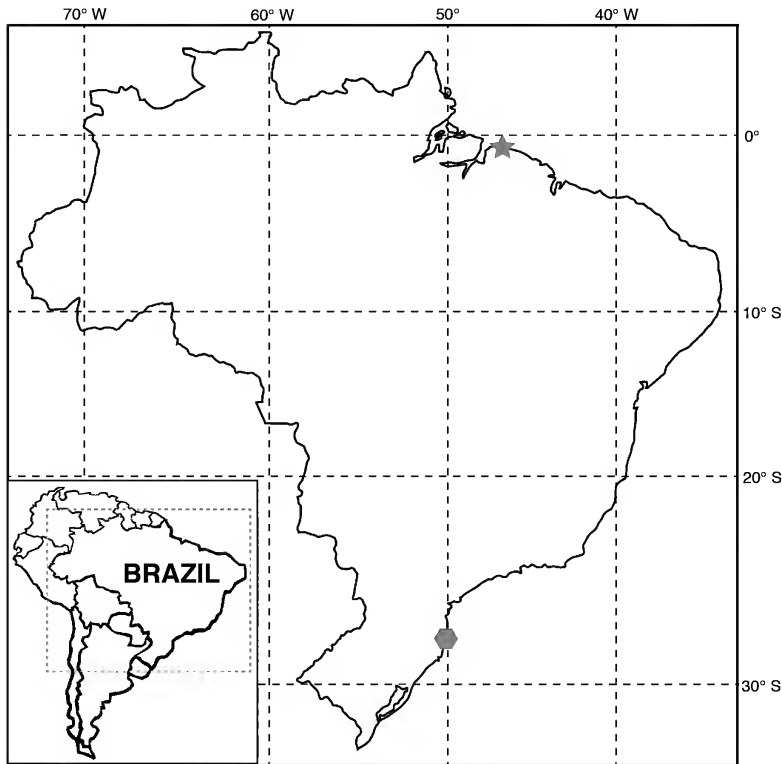
FIG. 1. Detail of collection sites for *Diadumene leucolena* (Verrill, 1866) (star) and type locality for *Diadumene manezinha*, sp. nov. (hexagon).

Diadumene leucolena Verrill, 1866

Figures 1–5, table 1

Sagartia leucolena Verrill, 1866: 336; 1868: 261–262; 1872: 436.
Cylista leucolena Andres, 1884: 157–158.
Sagartia (Thöe) leucolena Verrill, 1898: 495.
Diadumene leucolena Carlgren, 1950: 23–24; Hand, 1956: 223–230; Hand, 1957: 413.

MATERIAL: BRAZIL, Pará, Salinópolis, Praia do Farol Velho, 0°35′33′′S 47°19′29′′W, collected July 4, 2012, by L. Gusmão (0 m). MZUSP 002481 (10 specimens). *Material examined for comparison. Diadumene leucolena* (syntype) YPM 665 (8 specimens); Locality: New Haven Light, Long Island Sound, Connecticut (41.30 N 72.93W).

DIAGNOSIS: Individuals with conspicuous cinclides on raised columnar projections arranged in longitudinal rows on scapus. Fighting tentacles may be present. No anatomical irregularity due to asexual reproduction; 24 pairs of mesenteries in three cycles of mesenteries at midcolumn; third cycle never with distinct retractor or filaments. No *p*-mastigophores A on actinopharynx; acontia with one or two categories of *p*-mastigophores B2a (25.2–34.4 × 5.7–9.1 μm; 30.5–47.0 × 4.9–10.1μm).
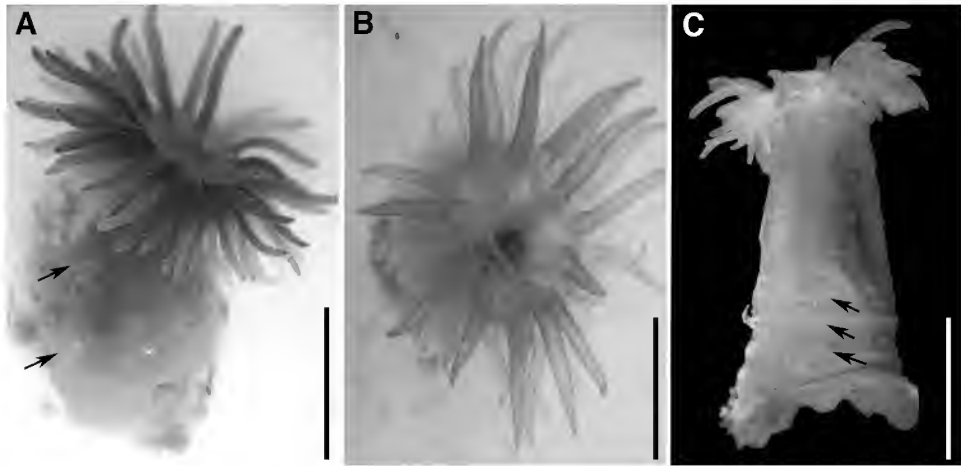
FIG. 2. External anatomy of *Diadumene leucolena* (Verrill, 1866). **A,** lateral view of living specimen showing cinclides with protruding acontia (arrows); **B,** oral view of living specimen; **C,** lateral view of preserved specimen showing scapus with cinclides on top of raised projections arranged in longitudinal rows (arrows). Scale bars: **A–B,** 3.0 mm; **C,** 2.5 mm.

EXTERNAL ANATOMY (fig. 2): Live and preserved specimens up to 6.0 mm in length (fig. 2A–C). Most preserved specimens with oral disc relaxed exhibiting visible tentacles (fig. 2C). Pedal disc adherent, flat, circular, diameter 2.0–4.0 mm in preserved specimens (fig. 2C). Column cylindrical, smooth, divided into scapus and capitulum separated by a collar (fig. 2C). Capitulum usually retracted into scapus, not easily visible in live (fig. 2A) or preserved specimens (fig. 2C); margin of capitulum tentaculate. Scapus with conspicuous cinclides positioned on top columnar projections through which acontia protrude (fig. 2A; arrows); cinclides arranged in 12 longitudinal rows with 3–6 cinclides per row distributed on proximal to distal scapus (fig. 2C; arrows). Column beige becoming light brown distally in live specimens, with mesenterial insertions visible as faint white lines on column from limbus to distal scapus (fig. 2A, C). Column diameter 3.0–4.0 mm and length 4.0–6.0 mm in preserved specimens. Oral disc circular, small, approximately as wide as column, with large brown central mouth in live

→

FIG. 3. Internal anatomy and microanatomy of *Diadumene leucolena* (Verrill, 1866). **A,** longitudinal section through distal column of a partially retracted specimen showing differentiation between scapus (dotted line) and capitulum (solid line) with limit between the two indicated by horizontal bar; **B,** cross section through actinopharynx showing glandular epidermis; **C,** cross section through actinopharynx showing well-differentiated siphonoglyph; **D,** cross section through feeding tentacle showing ectodermal longitudinal musculature (arrow); **E,** cross section through distal scapus at actinopharynx level showing the three cycles of mesenteries (indicated by numbers); note a raised projection on endocoel corresponding to a pair of directive mesenteries (arrow); **F,** cross section through scapus at distal actinopharynx level showing the three cycles of mesenteries (indicated by numbers); note larger, more developed retractors; **G,** cross section through distal scapus showing unequal development between mesenteries of a second cycle pair; **H,** cross section through proximal column showing detail of weak parietobasilar musculature in first cycle mesentery (arrow); **I,** detail of a fertile mesentery of second cycle showing oocytes. Abbreviations: **ac,** actinopharynx; **ca,** capitulum; **di,** directives; **ep,** epidermis; **ga,** gastrodermis; **oo,** oocytes; **sc,** scapus; **si,** siphonoglyph; **te,** tentacles. Scale bars: **A, D, G,** 0.1 mm; **B, C, I,** 0.07 mm; **E, F,** 0.4 mm; **H,** 0.012 mm.
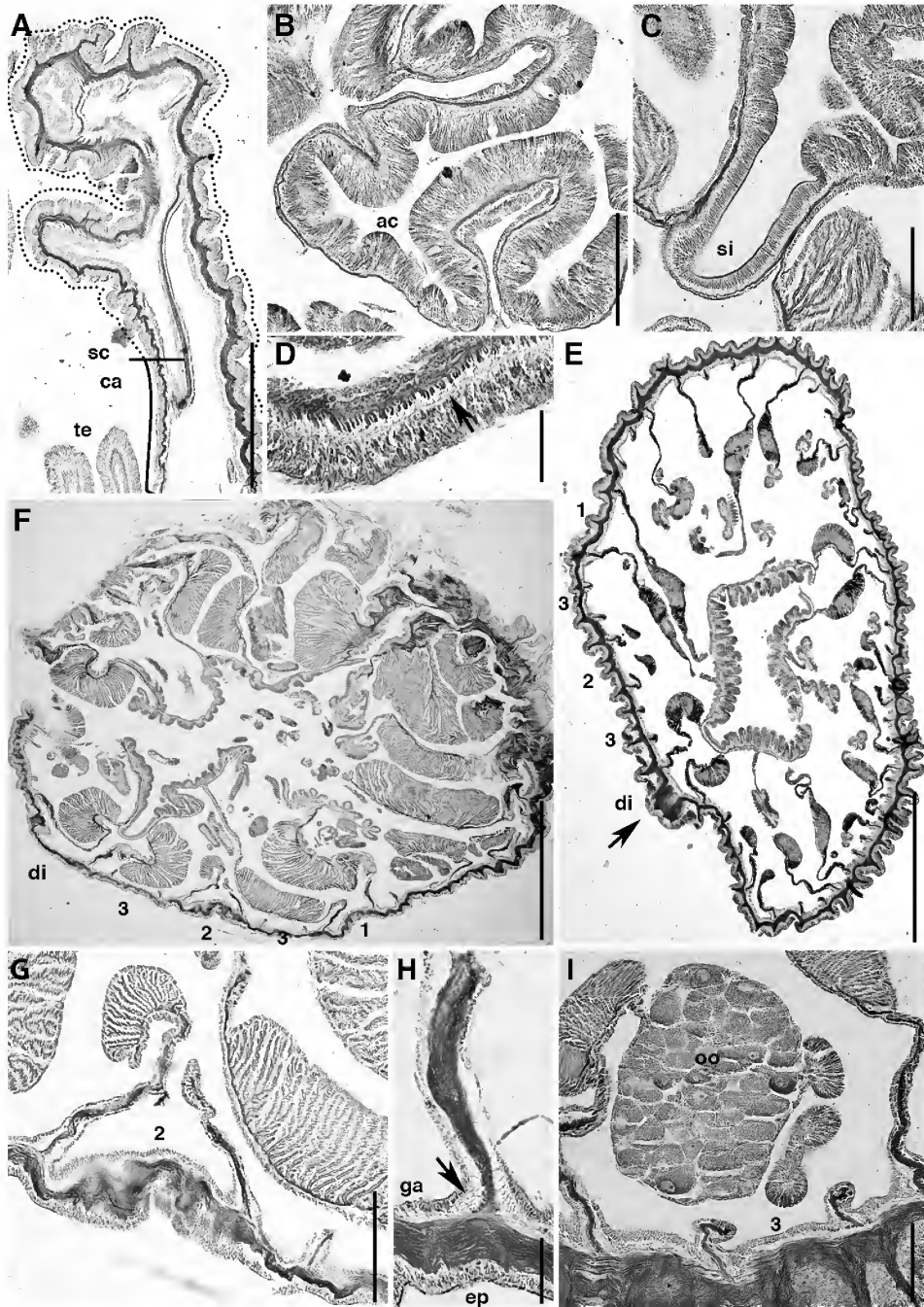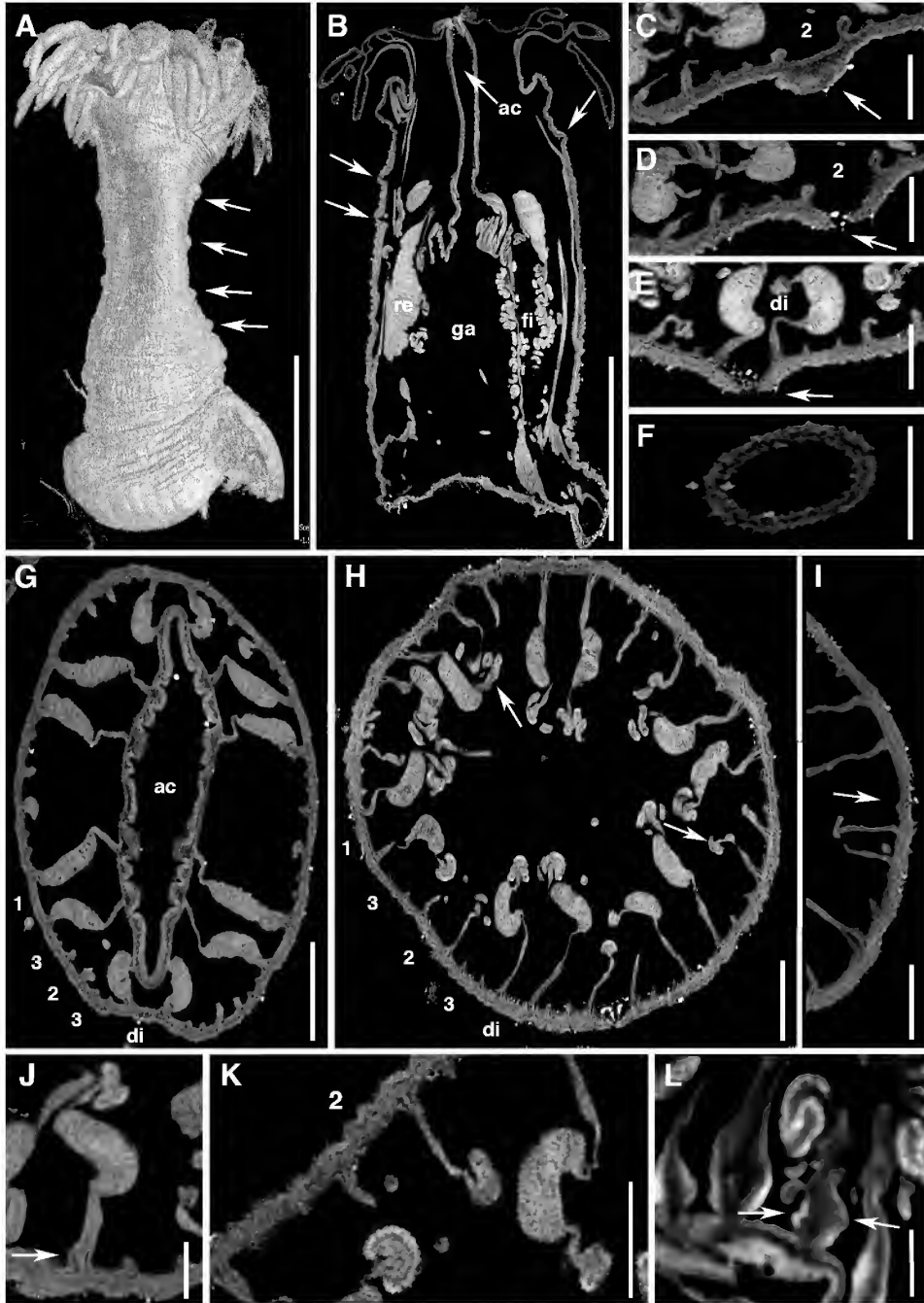
(fig. 2A, B) and preserved specimens. Oral disc yellow or brown with green markings at base of tentacles; diameter 2.0–4.5 mm in preserved specimens (fig. 2A, B). Tentacles 91–95, smooth, long, slender and pointed, arranged in four cycles (6+6+12+24+n) in outer half of oral disc in both live and preserved specimens (fig. 2A–C). Tentacles of first and second cycles brown or green with white markings along entire oral side (fig. 2A, B); tentacles of outer cycles white or translucent with no markings in live specimens (fig. 2A, B). All tentacles translucent white in preserved specimens (fig. 2C). Inner tentacles longer than outer ones in both live (fig. 2A, B) and preserved specimens (fig. 2C); longest tentacle up to 3 mm in live and preserved specimens. Fighting tentacles not visibly differentiated.

Internal anatomy, histology (figs. 3, 4): Body elongate in preserved specimens (fig. 4A) with wall thickness varying along column: all three body layers thicker in scapus than in capitulum; limit between scapus and capitulum gradual (fig. 4B) with transition zone visible in histological sections (fig. 3A). Cinclides positioned on top of raised projections with thick mesoglea (figs. 3E, 4C). Cinclides distributed in endocoels corresponding to first and second pairs of mesenteries (fig. 4C–E). Longitudinal endodermal musculature of column strong (fig. 3A). Actinopharynx up to 3.5 mm in length in largest specimen, approximately half of column's length (fig. 4B), longitudinally sulcated with 12 visible folds in distal part but more heavily folded proximally (fig. 4G); with thick and highly glandular epidermis (fig. 3B). Specimens with two differentiated siphonoglyphs (fig. 4G) exhibiting very thin gastrodermis and mesoglea but glandular epidermis as in actinopharynx (fig. 3C). Longitudinal musculature of tentacles ectodermal (fig. 3D).

Mesenteries hexamerously arranged in three cycles (6+6+12 = 24 pairs) spanning most of body length: first cycle perfect, including two pairs of directives, each associated with one siphonoglyph; second and third cycles imperfect (figs. 3E–F, 4G, H). Mesenteries of each second cycle pair unequally developed in specimens examined (figs. 3G, 4K). More mesenteries distally than proximally; mesenteries of third cycle may be absent proximally close to limbus (fig. 4I). Mesenteries of first and second cycles, including directives, fertile and with filaments; those of third cycle sterile and without filaments (fig. 3I). Species gonochoric: major axis of

FIG. 4. Micro-CT volumetric rendering and sections of *Diadumene leucolena* (Verrill, 1866). **A,** lateral view of the 3D rendering of a specimen showing cinclides in raised projections arranged in longitudinal rows (arrows); **B,** longitudinal section through whole specimen showing external and internal anatomy; notice raised projections on scapus (arrows); **C,** cross section through midscapus showing raised projection in endocoel corresponding to a second cycle pair of mesenteries (arrow); **D,** cross section through midscapus showing the cinclide (arrow) of the same second cycle pair of directive mesenteries shown in E ; **E,** cross section through midscapus showing cinclide in endocoel of a pair of directives (arrow); **F,** cross section through a feeding tentacle; **G,** cross section through distal scapus showing pairs of mesenteries of three cycles (indicated by numbers) including directive mesenteries; **H,** cross section through midscapus showing cycles of mesenteries (indicated by numbers); note filaments on mesenteries of first and some of second cycles (arrows); **I,** cross section through proximal scapus showing absence of mesenteries of third cycle (arrow); **J,** detail of a pair of mesenteries of first cycle with diffuse retractor and weak parietobasilar musculature (arrow); **K,** cross section through proximal scapus showing unequal development of a second cycle pair of mesenteries (indicated by number); **L,** cross section through pedal disc showing basilar musculature (arrow). Abbreviations: **ac,** actinopharynx; **di,** directive mesenteries; **fi,** filaments; **ga,** gastrovascular cavity; **re,** retractor. Scale bars: **A, B,** 2.0 mm; **C–E,** 0.25 mm; **F, J,** 0.2 mm; **G–I, K, L,** 0.5 mm.

Table 1. Size ranges of the cnidae of *Diadumene leucolena* (Verrill, 1866).
$\overline{X}$, mean; SD, standard deviation; S, proportion of specimens in which each cnidae was found; N, Total number of capsules measured; F, frequency; +++, very common; ++, common; +, rather common; -, rare

Categories	Range of length and width of capsules (µm)	$\overline{X} \pm$ SD	S	N	F
COLUMN					
Basitrichs I (A)	07.7–15.6 x 1.2–2.6	10.3±1.9 x 1.7±0.3	97	6/6	+++
Basitrichs II (B)	12.1–21.0 x 2.3–4.0	14.6±1.6 x 2.9±0.3	154	6/6	+++
p-mastigophores B2a (C)	07.6–23.5 x 2.4–5.1	14.7±4.9 x 3.8±0.7	50	6/6	+++
Holotrichs (D)	11.9–20.5 x 2.8–5.1	15.0±1.2 x 4.0±0.4	207	6/6	+++
TENTACLES					
Spirocysts (E)	11.0–21.8 x 2.2–5.0	16.0±1.9 x 3.5±0.5	264	6/6	+++
Basitrichs (F)	09.5–18.0 x 1.4–2.8	13.9±1.7 x 1.9±0.2	203	6/6	+++
p-mastigophores B2a II (G)	08.5–28.5 x 2.3–6.4	20.7±3.3 x 3.8±0.6	200	6/6	++
Holotrichs I (H)	11.9–17.2 x 2.4–3.8	14.1±1.1 x 3.1±0.3	115	6/6	+++
Holotrichs II (I)	15.4–22.4 x 2.1–3.5	17.9±1.2 x 2.8±0.3	122	3/6	++
ACTINOPHARYNX					
Basitrichs (J)	13.1–19.8 x 1.6–2.3	17.9±1.3 x 2.0±0.1	38	6/6	+
p-mastigophores B2a I (K)	08.8–10.9 x 2.4–3.4	10.1±0.9 x 2.8±0.5	04	3/6	-
p-mastigophores B2a II (L–M)	14.2–28.7 x 2.7–4.6	21.7±2.2 x 3.7±0.3	181	6/6	+
FILAMENT					
p-mastigophores B1 I (N)	06.9–15.5 x 3.4–5.4	9.6±1.3 x 4.1±0.4	107	5/5	+++
p-mastigophores B1 II (O)	11.1–19.1 x 3.8–5.3	15.4±1.7 x 4.4±0.4	100	5/5	++
p-mastigophores B2a I (P)	09.5–15.5 x 2.8–4.7	12.5±1.9x 3.7±0.4	55	4/5	+
p-mastigophores B2a II (Q)	18.7–31.8 x 3.3–5.0	23.6±2.5 x 4.1±0.5	55	4/5	+
ACONTIA					
Basitrichs (R)	12.0–21.3 x 1.4–2.4	13.8±0.9 x 1.9±0.1	352	6/6	+++
p-mastigophores B2a I (S)	25.2–34.4 x 5.7–9.1	30.0±1.6 x 6.7±0.7	90	6/6	++
p-mastigophores B2a II (T)	30.5–47.0 x 4.9–10.1	36.1±2.6x 6.6±0.9	356	6/6	+++

oocytes 13.6–48.0 µm in diameter; major axis of spermatic cysts 41.8–110.1 µm in diameter in specimens collected in July. Retractors of first and second cycles strong, most diffuse but some restricted (figs. 3E, F, 4G, H, J); those of third cycle very weak (figs. 3E–F, I, 4G, H, L). Parietobasilar musculature very weak in all mesenteries, with no free mesogleal flap (fig. 3H); not visible in micro-CT images (fig. 4K). Basilar musculature very weak (fig. 4L).

CNIDOM: Spirocysts, basitrichs, *p*-mastigophores B1, *p*-mastigophores B2a, and holotrichs. Acontia contain two types of nematocysts: basitrichs and *p*-mastigophores B2a. See figure 5 and table 1 for size and distribution.

DISTRIBUTION AND NATURAL HISTORY: *Diadumene leucolena* is known from San Francisco Bay, California (Hand, 1956) on the West Coast of the United States and from Woods Hole, Massachusetts, to Beaufort, North Carolina (see Verrill et al., 1873; McMurrich, 1887; Verrill,
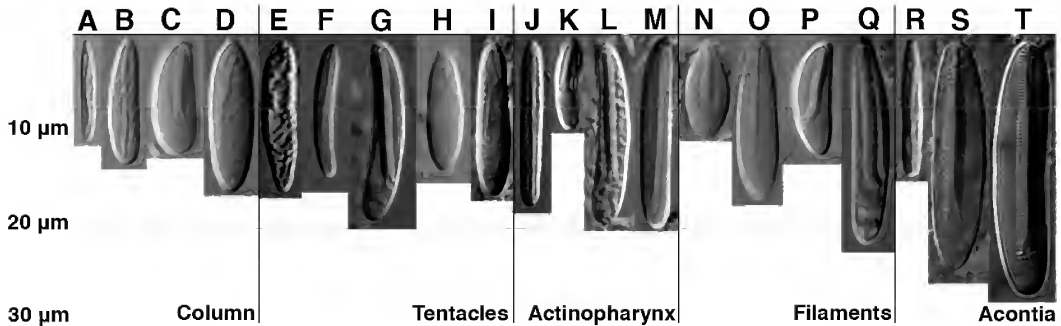
FIG. 5. Cnidom of *Diadumene leucolena* (Verrill, 1866). **A, B, F, J, R,** basitrich. **C, G, K, L, M, P, Q, S, T,** *p*–mastigophore B2a. **D, H, I,** holotrich. **E,** spirocyst. **N, O,** *p*–mastigophore B1.

1898; Hand, 1956), on the East Coast of the United States. In Brazil, *D. leucolena* was collected in Praia do Farol Velho (Salinópolis, Pará) and observed but collected for molecular study only in Praia do Atalaia (Salinópolis, Pará). This species can be abundant locally and is found attached to the underside of rocks or in crevices in the lower intertidal.

Diadumene manezinha, new species

Figures 1, 6–9, table 2

Material: Holotype. BRAZIL, Santa Catarina, Florianópolis, dock located in the Barra da Lagoa Channel, 27°35′4.49″S; 48° 26′10.45″W, collected November 19, 2011, by L. Gusmão and A. Grajales (0 m). MZUSP 002504 (1 specimen). *Material examined for comparison: Diadumene neozelanica* ZMUC ANT-000076 (4 specimens; syntypes); Locality: New Zealand, Kaipara, North Island, Slipper Island, -37.05, 175.94, collected January 8, 1915, by Th. Mortensen "Hinemoa" (Th. Mortensen's Pacific Expedition). *Diadumene* sp. MNRJ 7055 (6 specimens); Locality: Flutuante da Vaca, RJ, Brazil, collected November 1, 1990, by D.O. Pires. *Diadumene* sp. (8 specimens); Locality: Praia do Boqueirão, Ilha do Governador, RJ, Brazil, collected August 10, 1987, by INSB-E. Martins. *Diadumene* sp. MNRJ 7169 (20 specimens); Locality: Praia da Guanabara, Ilha do Governador, RJ, Brazil, collected July 11, 1987, by INSB-E. Martins.

Diagnosis: Individuals with inconspicuous cinclides arranged in longitudinal rows on scapus. Fighting tentacles with holotrichs of two types may be present. No anatomical irregularity due to asexual reproduction; 24 pairs of mesenteries in three cycles of mesenteries at midcolumn; third cycle never with distinct retractor or filaments. Actinopharynx with small *p*-mastigophores A (18–38.7 × 2.7–5.0 μm); acontia with three categories of *p*-mastigophores B2a (20.9–33.2 × 4.0–5.4 μm; 35.0–53.9 × 5.8–10.0 μm; 57–69.0 × 7.9–10.7 μm).

External anatomy (fig. 6): Live and preserved specimens up to 11.0 mm in length (fig. 6A–C). Most preserved specimens with oral disc relaxed exhibiting visible tentacles (fig. 6B–D). Pedal disc flat, circular, adherent, diameter 1.5–5.5 mm in diameter in preserved specimens (fig. 6A–C). Column cylindrical, smooth, divided into long scapus and short capitulum (fig. 6A–C). Capitulum usually not distinct in fully extended live specimens (fig. 6A) and well-
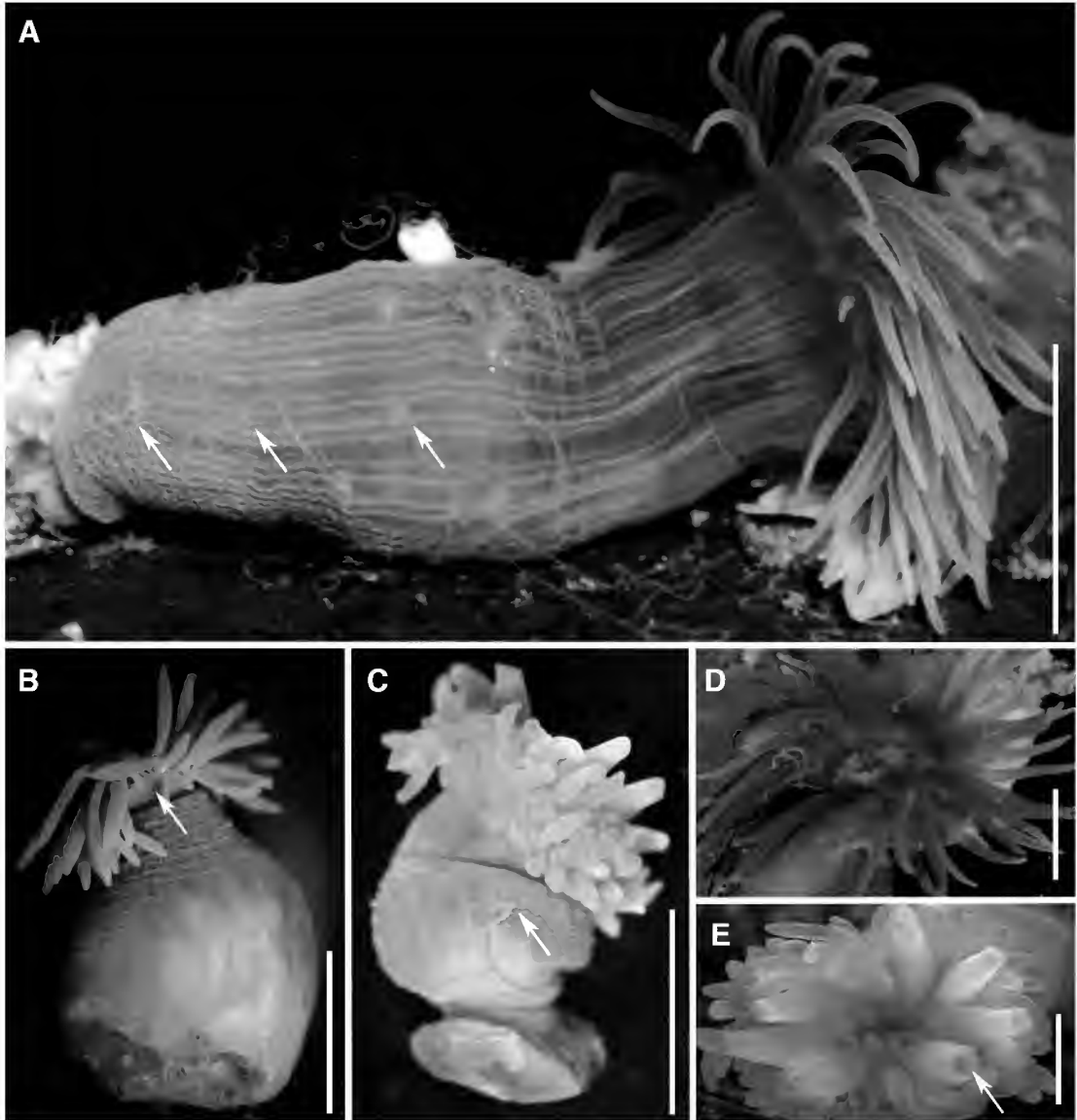
FIG. 6. External anatomy of *Diadumene manezinha*, sp. nov. **A,** lateral view of an extended living specimen showing row of cinclides (arrows); **B,** lateral view of preserved specimen showing capitulum retracted into scapus (arrow); **C,** lateral view of preserved specimen showing cinclide on scapus with protruding acontium (arrow) **D,** oral view of living specimen; **E,** oral view of preserved specimen showing fighting tentacles; notice fighting tentacle with autotomized tip (arrow). Scale bars: **A,** 3.0 mm; **B,** 2.5 mm; **C,** 3.5 mm; **D,** 1.5 mm; **E,** 2.0 mm.

relaxed preserved ones (fig. 6C) or retracted into scapus in contracted preserved ones (fig. 6B); margin of capitulum tentaculate. Scapus with inconspicuous cinclides not positioned on top of raised projections (fig. 6A–C); cinclides arranged in 12 longitudinal rows with 2–4 cinclides per row distributed on proximal to distal scapus but more conspicuous in proximal half of scapus in live (fig. 6A) and preserved specimens (fig. 6C). Column olive green with mesenterial insertions visible as beige lines on column from limbus to distal scapus (fig. 6A–C). Column diameter 2.0–7.0 mm and length 1.0–11.0 mm in preserved specimens. Oral disc circular, small, as wide or slightly wider than column, olive green becoming lighter close to base of inner tentacles with large orange, central mouth exhibiting 12 distinct lobes in live specimens (fig. 6D). Oral disc diameter 1.0–4.5 mm in preserved specimens (fig. 6E). Tentacles 89–92, smooth, long, slender and pointed, arranged in five cycles ($6+6+12+24+n$) in outer half of oral disc in both live (fig. 6D) and preserved specimens (fig. 6E). Tentacles of first and second cycles olive green somewhat darker than the light green or yellow tentacles in outer cycles (fig. 6A, D); tentacles with no markings in live specimens (fig. 6D). All tentacles translucent beige in preserved specimens (fig. 6B, C, E). Inner tentacles longer than outer ones in both live (fig. 6A, D) and preserved specimens (fig. 6B, C, E); longest tentacle up to 3 mm in live and preserved specimens. Fighting tentacles large, with blunt tip and broad base, exhibiting different color from feeding tentacles, observed in three preserved specimens (fig. 6E). Six fighting tentacles of first cycle observed in two specimens; six tentacles of first cycle and one of second cycle observed in one specimen (fig. 6E). One fighting tentacle of the specimen with seven of them had its tip autotomized (fig. 6E, arrow).

INTERNAL ANATOMY AND HISTOLOGY (figs. 7, 8): Body short and broad in preserved specimens (fig. 8A) with wall thickness varying along column: all three body layers thicker in scapus than capitulum; limit between scapus and capitulum gradual (fig. 8B, C) with transition zone visible in histological sections (figs. 7A). Cinclides mostly inconspicuous, not positioned on top of raised projections, but easily observed in histological sections (fig. 7B). Cinclides distributed in endocoels corresponding to first and second cycle pairs of mesenteries. Longitudinal endodermal musculature of column strong (fig. 7C). Actinopharynx up to 2 mm in length, approximately one third of column's length (fig. 8B), longitudinally sulcated throughout; with thick and highly glandular epidermis (fig. 7E). Specimens with two differentiated siphonoglyphs (fig. 8E) exhibiting thin gastrodermis and mesoglea, but glandular epidermis as in actinopharynx (fig. 7E). Longitudinal musculature of tentacles ectodermal (figs. 7D, 8D).

Mesenteries hexamerously arranged in three cycles ($6+6+12 = 24$ pairs) spanning most of body length: first cycle perfect, including two pairs of directives, each associated with one siphonoglyph (fig. 8E); second and third cycles imperfect (fig. 8E). A few specimens exhibited irregularities in the distribution of mesenteries but only proximally (fig. 8F, G). More mesenteries distally than proximally (fig. 8G). All mesenteries of first and second cycles, including directives, fertile and with filaments (figs. 7A, 8F); those of third cycle sterile and without filaments (figs. 7F, 8F). Species gonochoric: major axis of oocytes 16.4–31.3 μm in diameter; major axis of spermatic cysts 87.0–221.0 μm in diameter in specimens collected in November. Retractors of first and second cycles strong, most diffuse but some restricted (figs. 7F, 8F); those of
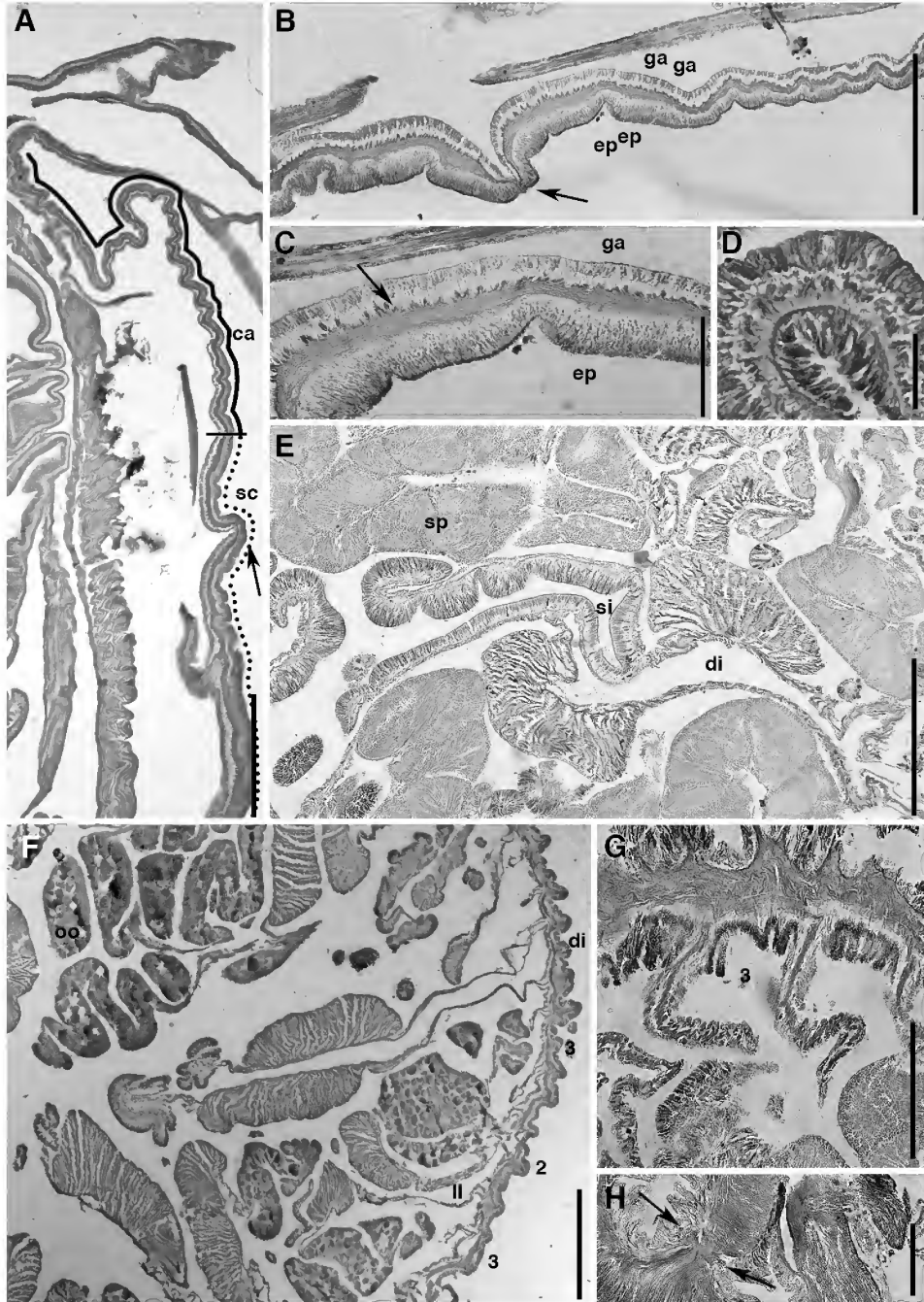
third cycle very weak (figs. 7F, G, 8E, F). Parietobasilar musculature very weak in all mesenteries, with no free mesogleal flap (fig. 7G); not visible in micro-CT images (fig. 8I). Basilar musculature of mesenteries weak (figs. 7H, 8J).

Cnidom (fig. 9): Spirocysts, basitrichs, *p*-mastigophores A, *p*-mastigophores B1, *p*-mastigophores B2a, and holotrichs. Acontia contain two types of nematocysts: basitrichs and *p*-mastigophores B2a. See figure 9 and table 2 for size and distribution.

Distribution and natural history: Specimens were collected attached to a rope tied to a dock in the channel that connects Lagoa da Conceição to Praia da Barra da Lagoa (closer to the latter). Individuals formed large aggregations with specimens of variable sizes.

Etymology: The species epithet refers to the popular name of inhabitants of the type locality of the species, Florianópolis, Santa Catarina, Brazil (i.e., *manezinhos da ilha*).

Molecular phylogenetic analysis: Similar sequence lengths were obtained for all *Diadumene* specimens studied: approximately 600 bp were sequenced for 12S, 400 bp were sequenced for 16S mitochondrial rDNA, while approximately 1500 bp were obtained for 18S nuclear rDNA. The phylogenetic relationships recovered are depicted in figure 10: within Metridioidea, clade Metridina of Rodríguez et al. (2012) was recovered with high support (99%), and included a well-supported monophyletic Diadumenidae (100%) sister to a clade containing members of Metridiidae and Acricoactinidae Larson, 2016. The genus *Diadumene* was recovered as monophyletic with high support (100%) and was composed of two major clades: one formed by the two specimens of *D. leucolena* (from the coasts of Brazil and the United States) found as sister taxa to *D. manezinha* with high support (100%), and the second formed by the remaining species of *Diadumene* included in this study (*D. cincta*, *D. paranaensis*, *Diadumene* sp., and *D. lineata*).

Micro-CT scanning: Different tissue types were successfully stained with osmium tetroxide and micro-CT scanning resulted in high-contrast images consistent between the two species of *Diadumene* examined (figs. 4, 8). Fine details of external and internal anatomical characters traditionally used in the taxonomy of sea anemones were readily observed in the 2D micro-CT images and 3D volumetric renderings of each species.

2D micro-CT reconstructions: Most external anatomical features were easily identified in the 2D micro-CT images: pedal disc morphology (figs. 4B, 8B), column morphology and its division into scapus and capitulum (figs. 4B, 8B, C), columnar specializations (i.e., cinclides,

---

FIG. 7. Internal anatomy and microanatomy of *Diadumene manezinha*, sp. nov. **A,** longitudinal section through column showing differentiation between scapus (dotted line) and capitulum (solid line) with limit between the two indicated by horizontal bar; notice cinclide on scapus (arrow); **B,** longitudinal section through distal column showing a cinclide in detail (arrow); **C,** longitudinal section through mid-scapus showing endodermal musculature (arrow); **D,** cross section through a feeding tentacle showing ectodermal longitudinal musculature; **E,** cross section through distal scapus showing retractors of directive mesenteries and spermatic cysts; **F,** cross section through proximal scapus showing cycles of mesenteries (indicated by numbers) and a pair of directives; note mesenteries of first and second cycles with oocytes; **G,** detail of mesenteries of third cycle (indicated by number); **H,** cross section through pedal disc showing basilar musculature (arrows). Abbreviations: **ca,** capitulum; **di,** directive mesenteries; **ep,** epidermis; **ga,** gastrodermis; **oo,** oocytes; **sc,** scapus; **si,** siphonoglyph; **sp,** spermatic cysts. Scale bars: **A,** 0.25 mm; **B, C,** 0.05 mm; **D,** 0.025 mm; **E, G, H,** 0.2 mm; **F,** 0.4 mm.
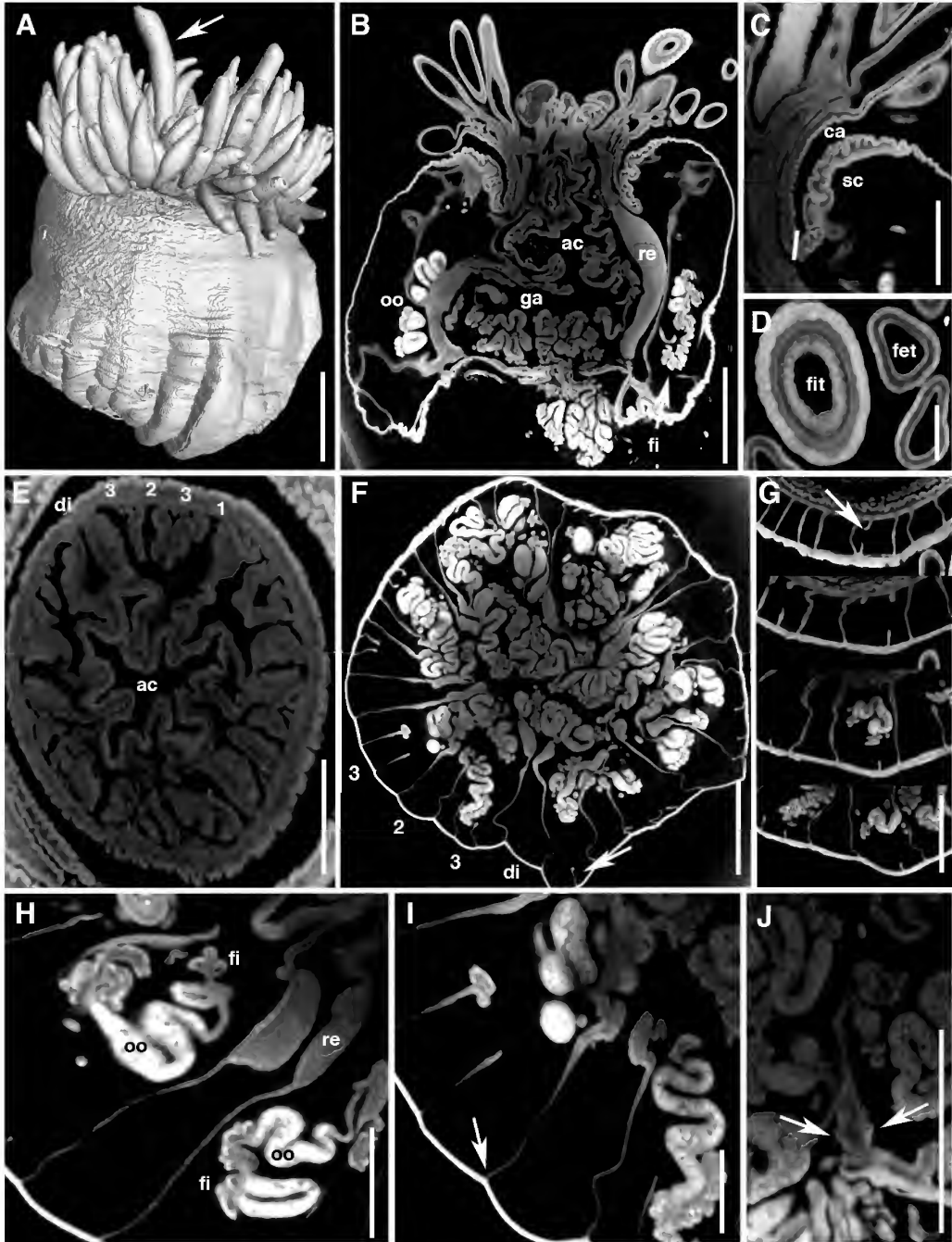
fig. 4B–E) and feeding (figs. 4F, 8D) and fighting tentacles (fig. 8D). The tentacles of *Diadumene leucolena*, however, exhibited low contrast (fig. 4F). The ectodermal musculature of tentacles could not be not visualized in the images (figs. 4F, 8D). The distribution of cinclides in endocoels of first and second cycles was particularly easy to establish in micro-CT images from *D. leucolena* (fig. 4C–E). Internal features were also readily visualized in micro-CT scans, including actinopharynx size and morphology (figs. 4B, G, 8B, E), number and distribution of siphonoglyphs (figs. 4G, 8E), presence and distribution of filaments (figs. 4B, H, 8B, F), and gametogenic tissue in *D. manezinha* (fig. 8B, F, H, I), the only species found fertile. The gametogenic tissue exhibited particularly high contrast to osmium tetroxide, which facilitated the recognition of fertility patterns in the specimen of *D. manezinha* scanned. Although general musculature shape and morphology was accurately established from micro-CT scans for both species examined (e.g., retractors, figs. 4B, G, H, J, 8E, F, H, I; basilar musculature, figs. 4L, 8J), the resolution of the images obtained was not sufficient to visualize details of musculature (e.g., number and branching pattern in retractors).

3D MICRO-CT RECONSTRUCTIONS: All external features observed in the 2D micro-CT scans were also seen in the computer-aided 3D reconstructions for *Diadumene leucolena* and *D. manezinha* (figs. 4A, 8A). Column morphology and its division into scapus and capitulum was accurately visualized only for *D. leucolena* (fig. 4A), due to the degree of contraction seen in the specimen of *D. manezinha* scanned (fig. 8A). Likewise, while the morphology, number, and arrangement of feeding tentacles and fighting tentacles in *D. manezinha* (fig. 8A, D), and feeding tentacles of *D. leucolena* was easily observed in the 3D reconstruction (fig. 4A), the tentacles of *D. leucolena* displayed lower resolution in certain regions corresponding to areas where 2D micro-CT images exhibited low contrast (fig. 4F). Similarly, all internal characters observed in the micro-CT images were observed in the 3D reconstructions and certain characters were especially prominent as a result of the tridimensionality from the 3D reconstructions: mesentery growth pattern (fig. 8I), number of mesenteries distally and proximally (figs. 4G–I, 8E–G), distribution of filaments (figs. 4H, 8F), and gametogenic tissue (fig. 8F). In addition, establishment of characters such as position of cinclides (e.g., endocoels of first and second cycles in *D.*

FIG. 8. Micro-CT volumetric rendering and sections of *Diadumene manezinha*, sp. nov. **A,** lateral view of 3D rendering of whole specimen showing external anatomy showing; note the long fighting tentacle (arrow); **B,** longitudinal section through whole specimen showing external and internal anatomy; **C,** cross section through distal column showing detail of capitulum; **D,** cross section through fighting tentacle and two feeding tentacles; **E,** cross section through distal scapus showing pairs of mesenteries of three cycles (indicated by numbers) including directive mesenteries; **F,** cross section through midscapus showing cycles of mesenteries (indicated by numbers) and gonads on first and second cycles; notice unpaired mesentery of third cycle (arrow); **G,** cross section through column at different levels showing unpaired mesentery of third cycle only distally (arrow); **H,** cross section through proximal scapus showing a pair of mesenteries of first cycle with diffuse retractor and no visible parietobasilar musculature; notice oocytes on pairs of mesenteries of second cycle; **I,** cross section through proximal scapus showing detail of a pair of mesenteries of second and third cycles; parietobasilar musculature is not visible (arrow); **J,** cross section through pedal disc showing basilar musculature (arrows). Abbreviations: **ac,** actinopharynx; **ca,** capitulum; **di,** directive mesenteries; **fe,** feeding tentacle; **fi,** filament; **fit,** fighting tentacle; **ga,** gastrovascular cavity; **oo,** oocytes; **re,** retractor musculature; **sc,** scapus. Scale bars: **A,** 1.5 mm; **B,** 2.0 mm; **C, D,** 0.4 mm; **E, G–J,** 1.0 mm; **F,** 2.0 mm; **I,** 0.8 mm.

Table 2. Size ranges of the cnidae of *Diadumene manezinha*, sp. nov.
$\overline{X}$, mean; SD, standard deviation; S, proportion of specimens in which each cnidae was found; N, Total number of capsules measured; F, frequency; +++, very common; ++, common; +, rather common; -, rare.

| Categories	Range of length and width of capsules (µm)	$\overline{X} \pm$ SD	S	N	F	*Diadumene neozelanica* (ZMUC-ANT000076)
COLUMN						
Basitrichs I (A)	08.1–16.0 x 1.3–2.5	10.5±1.1 x 1.8±0.2	186	6/6	+++	13.1–17.0 x 1.8–2.8
Basitrichs II (B)	11.6–21.5 x 2.3–4.5	17.3±2.0 x 3.4±0.4	289	6/6	+++	13.8–24.1 x 3.0–3.9
p-mastigophores B2a (C–D)	09.7–27.3 x 2.6–5.5	16.6±4.2 x 4.3±0.6	399	6/6	+++	07.1–23.0 x 2.8–5.3
Holotrichs (E)	12.0–17.6 x 3.2–4.9	14.8±1.2 x 3.9±0.4	61	5/6	++	14.1–17.1 x 4.6–6.0
TENTACLES						
Spirocysts (F)	12.3–26.0 x 2.1–6.0	19.9±2.9 x 3.5±0.7	269	5/5	+++	10.0–17.0 x 1.9–5.2
Basitrichs G	08.5–22.0 x 1.4–4.0	17.4±3.2 x 2.2±0.5	153	5/5	+++	11.7–19.7 x 1.8–2.4
p-mastigophores B2a (H)	15.3–35.6 x 2.7–5.4	29.0±4.1 x 4.5±0.5	185	5/5	+++	07.7–15.4 x 2.3–4.2
FIGHTING TENTACLES						
Holotrichs I (I)	13.7–14.6 x 3.2–3.8	14.1±0.5 x 3.5±0.3	52	3/5	++	22.6–38.4 x 4.1–5.6
Holotrichs II (J)	17.0–29.0 x 3.0–4.9	20.9±2.3 x 3.3±0.4	65	3/5	++	21.2–36.3 x 8.3–12.5
ACTINOPHARYNX						
Basitrichs (K)	10.6–24.4 x 1.4–2.8	19.4±1.9 x 2.0±0.2	181	6/6	+++	14.2–28.6 x 2.0–3.0
p-mastigophores A (L)	18.0–38.7 x 3.0–5.6	26.5±5.5 x 4.1±0.6	87	6/6	++	14.1–21.7 x 2.2–3.9
p-mastigophores B2a I (M)	08.9–20.0 x 2.7–5.0	14.5±2.3 x 3.7±0.5	75	5/5	++	10.4–18.0 x 2.7–4.4
p-mastigophores B2a II (N–O)	16.9–42.0 x 3.0–6.0	26.8±2.9 x 4.2±0.6	313	6/6	+++	21.6–32.4 x 2.8–4.9
FILAMENT						
Basitrichs (P)	08.4–20.4 x 1.3–3.5	11.1±3.6 x 1.8±0.6	55	4/5	+	11.3–15.7 x 1.3–3.0
p-mastigophores A	-					17.2–19.4 x 3.7–3.9
p-mastigophores B1 I (Q)	5.8–10.4 x 3.2–5.4	8.4±0.9 x 4.2±0.3	246	5/5	+++	09.1–13.5 x 3.7–5.4
p-mastigophores B1 II (R)	11.6–19.6 x 3.3–5.7	15.0±1.4 x 4.4±0.4	129	5/5	+++	15.2–22.7 x 4.3–6.0
p-mastigophores B2a (S)	10.5–33.9 x 3.1–5.2	15.4±4.0 x 3.8±0.4	100	5/5	++	10.1–23.6 x 2.7–4.7
p-mastigophores B2a	-					30.8–39.7 x 4.8–5.8
ACONTIA						
Basitrichs (T)	09.7–16.8 x 1.2–3.0	14.3±0.4 x 2.1±0.4	124	6/6	+++	09.2–18.7 x 2.1–3.4
p-mastigophores B1	-					17.0–23.0 x 2.5–3.2
p-mastigophores B2a I (U)	20.9–33.2 x 4.0–5.4	26.7±3.1 x 4.9±0.5	110	6/6	++	-
p-mastigophores B2a II (V)	35.0–53.9 x 5.8–10.0	44.4±3.5 x 7.5±0.9	170	6/6	+++	-
p-mastigophores B2a III (X)	57.0–69.2 x 7.9–10.7	61.7±3.1 x 9.1±0.7	54	6/6	+	51.2–77.0 x 5.1–8.2
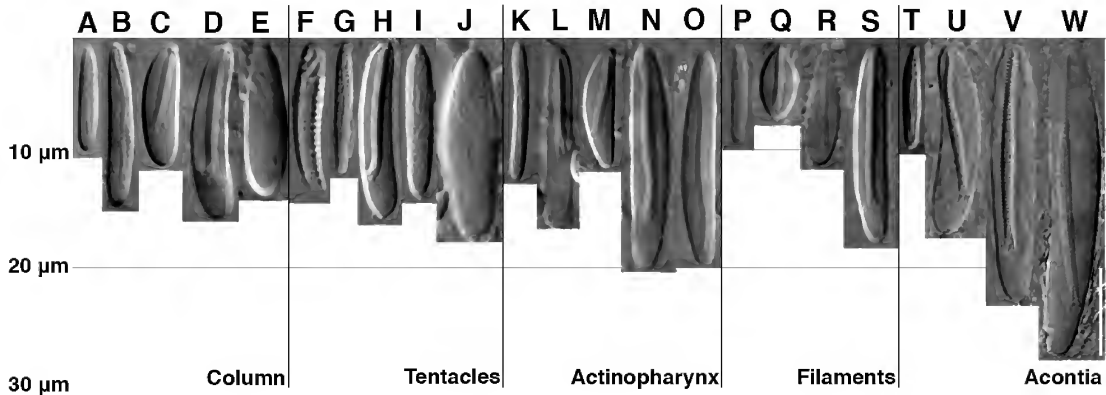
FIG. 9. Cnidom of *Diadumene manezinha*, sp. nov. **A, B, G, K, P, T,** basitrich; **C, D, H, M, N, O, S, U, V, W,** *p*-mastigophore B2a; **E, I, J,** holotrich; **F,** spirocyst; **L,** *p*-mastigophore A; **Q, R,** *p*-mastigophore B1. Scale bar: 15 μm.

leucolena) was considerably facilitated by the use of virtual sections from 3D volumetric renderings (fig. 4A–E).

ARTIFACTS: Artifacts did not affect the accuracy of micro-CT images, posterior 3D representation, or establishment of characters for the two species examined. Among the artifacts, we observed low contrast of micro-CT images of the gastrovascular cavity core in the specimen of *Diadumene manezinha* compared with more peripheral areas (fig. 8B, E, F). Similarly, micro-CT images of the distal part of the column corresponding to the capitulum of *D. manezinha* suggested imperfect penetration of the stain in this specimen (fig. 8E). Probably resulting from imperfect penetration of the stain, air pockets inside the gastrovascular cavity of *D. leucolena* were seen as black voids in the micro-CT images (fig. 8B). Air pockets, however, were small and did not affect the morphology of internal features or compromise the recognition or orientation of surrounding anatomical characters. A more pervasive artifact related to air pockets caused a greater technical problem for the method: movement of the specimen during scanning. Air pockets created inside the specimen before scanning may result in slight movements if the specimen is not securely positioned, leading to blurry images and posterior problems in the alignment of multiple scans (results not shown).

DISCUSSION

FAMILIAL AND GENERIC PLACEMENT: The combination of the presence of *p*-mastigophores B2a and basitrichs in the acontia and no marginal sphincter musculature places *Diadumene leucolena* and *D. manezinha* in the family Diadumenidae. The two species can be easily differentiated from members of families with similar morphology by the mesogleal sphincter and *b*-mastigophores in addition to *p*-mastigophores B2a in acontia of Metridiidae and by presence of only basitrichs in the acontia of Acricoactinidae.

All examined specimens of *Diadumene leucolena* and *D. manezinha* exhibited features that in combination characterize *Diadumene* (see genus diagnosis). In addition, fighting tentacles

were morphologically differentiated in three out of the 20 specimens of *D. manezinha* examined. Unlike feeding tentacles, fighting tentacles were opaque, thicker, and with blunt tips as described by Williams (1975). A single fighting tentacle lacked part of its tip (fig. 6E), which might suggest autotomization, a known result of agonistic behavior (Williams, 1975; Purcell, 1977). Absence of visibly differentiated fighting tentacles in most specimens of *D. manezinha* and all specimens of *D. leucolena* is not exceptional within Diadumenidae, as these structures have never been observed in some species (e.g., *D. fransciscana* and *D. lighti*) and when present may appear in frequencies as low as 1.7% in some populations (e.g., populations of *D. lineata* in England: Williams, 1975). Likewise, fighting tentacles are ephemeral during an individual's lifespan, being induced by territorial threats from non-clonemates (Williams, 1975; Purcell, 1977; Watson and Mariscal, 1983a; Östman et al., 2010a) and restricted to individuals along the border of an aggregation facing other aggregates (Purcell, 1977; Purcell and Kitting, 1982). The reversal from fighting tentacles is also possible, being correlated with isolation of individuals to areas with non-clonemates (Hand, 1956) or an animal's nutritional state (Williams, 1975; Hand, 1956). In both instances, a change in nematocyst content accompanies the transformation (Purcell, 1977; Watson and Mariscal, 1983a).

Despite finding holotrichs of two distinct morphologies in inner tentacles of specimens of *Diadumene leucolena* from Brazil (fig. 5H, I), these tentacles were not visibly differentiated into fighting tentacles. The holotrichs seen in tentacles of *D. leucolena*, however, are not the typical ones seen in fighting tentacles of *Diadumene*, but divided into two types of holotrichs: the first type (fig. 5H) similar to those described by Excoffon et al. (2004) as anisorhize haplonemes for feeding tentacles of *D. lineata* and by Östman et al. (2010a) as isorhizas for *Metridium senile* (Linneus, 1761) (Östman et al., 2010a) and a second type (fig. 5I) similar to the slender ones seen in fighting tentacles of *Diadumene* species (e.g., *D. lineata*, Kovtun et al., 2012: fig. 5e), including *D. manezinha* (fig. 9I). Unfortunately, we did not observe undischarged capsules of either type of holotrich and cannot further classify them into isorhizas or anisorhizas. In addition to having holotrichs, tentacles exhibited cnidae typical of feeding tentacles (i.e., spirocysts, basitrichs, and *p*-mastigophores B2a; fig. 5E–G, respectively), which is usually rare in fighting tentacles (Stephenson, 1935; Williams, 1975; Purcell, 1977; Watson and Mariscal, 1983a). This might suggest that feeding tentacles seen in specimens of *D. leucolena* were either in the early stages of transforming into fighting tentacles, given the predominance of small holotrichs over larger ones characteristic of later stages (table 1), or were in the process of reverting from fighting tentacles to feeding tentacles (see Watson and Mariscal, 1983b). Similarly, Carlgren (1950) found cnidae typical of fighting tentacles in the tips of tentacles of *D. leucolena* that were not visibly differentiated from other feeding tentacles. Fukui (1986) also noted that fighting tentacles of *D. lineata* were similar to feeding tentacles in coloration and shape when contracted, becoming differentiated only when expanded in the manner characteristic of these structures. Likewise, Larson and Daly (2015) hypothesized that a non-differentiated tentacle with holotrichs and rare spirocysts in one specimen of the actineoidean *Epiactis ritteri* Torrey, 1902, is a fighting tentacle. Alternatively, it is possible that contamination of other parts of the tentacle with cnidae typical of feeding tentacles occurred during sampling of the tip of tentacles in which holotrichs are concentrated in fighting tentacles (Watson and Mariscal, 1983a).

Given the transient nature and low frequency of fighting tentacles in populations of species that possess them (e.g., Hand, 1956; Williams, 1975), we agree with others (e.g., Hand, 1956; Riemann-Zürneck, 1975; Williams, 1975; Manuel, 1981; den Hartog and Ates, 2011) and recommend that presence of fighting tentacles be taken in combination with other characters to more effectively distinguish members of Diadumenidae from other metridioidean families. Nevertheless, we maintain the presence of fighting tentacles in the diagnosis of family Diadumenidae given its uniqueness within Actiniaria, as a way to help identify species that exhibit them. We infer that fighting tentacles are present in all species of *Diadumene* and not absent, but unobserved in populations of *D. franciscana* and *D. lighti*. The fact that for more than 75 years thousands of specimens from several populations from Japan, North America, and Europe of *D. lineata* were examined (e.g., Sephenson, 1925, 1935; Uchida, 1932; Hand, 1956) before Williams (1975) confirmed the presence of fighting tentacles in populations from Plymouth (England) and Misaki (Japan) suggests this could be the case for *D. fransciscana* and *D. lighti*. That fighting tentacles may be absent in *D. lineata* populations undergoing frequent pedal laceration while present in high abundance in other populations with frequent sexual reproduction (Fukui, 1986) might provide an avenue for exploration of the cause of their absence in other species and populations. In addition to the eight species of Diadumenidae, however, only nine species in five metridioidean families exhibit fighting tentacles with holotrichs: *Metridium senile* (Metridiidae) (Williams, 1975; Hand, 1956); *Cereus pedunculatus* (Pennant, 1777), *Sagartia elegans* (Dalyell, 1848), *Sagartia troglodytes* (Price in Johnston, 1847) (Williams, 1975), *Verrillactis paguri* (Verrill, 1869a), and *Habrosanthus bathamae* Cutress, 1961 (Sagartiidae Gosse, 1858); *Flosmaris bathamae* Hand, 1961(Andvakiidae Danielssen, 1890, sensu Rodríguez et. al., 2012); *Sagartiomorphe carlgreni* Kwietniewski, 1898 (Sagartiomorphidae Carlgren, 1934) (Carlgren, 1940); *Tricnidactis errans* Pires, 1987 (Haliplanellidae Hand, 1956). Despite the obvious polyphyly of Sagartiidae (Daly et al., 2008; Rodríguez et al., 2012, 2014), a close relationship among Metridiidae, Diadumenidae, and some sagartiids (e.g., *V. paguri, S. troglodytes*) with fighting tentacles has been recovered in phylogenetic analyses (Gusmão and Daly, 2010; Rodríguez et al., 2012, 2014), which suggests fighting tentacles have putatively independently evolved fewer times than suspected. In addition to metridioideans, tentacles with holotrichs have been found in actinioideans belonging to family Actiniidae Rafinesque, 1815: *Epiactis japonica* (Verrill, 1869a) (as *Cnidopus japonicus*: Sanamyan and Sanamyan, 1998; Larson and Daly, 2015), Pacific populations of *Aulactinia stella* (Verrill, 1864) (Sanamyan and Sanamyan, 1998), and *Epiactis ritteri* Torrey, 1902 (Larson and Daly, 2015). Earlier, Fautin and Chia (1986) found holotrichs in tentacles of *Epiactis lisbethae* Fautin and Chia, 1986, *Epiactis fernaldi* Fautin and Chia, 1986, and *Epiactis prolifera* Verrill, 1869b. Similarly, Sanamyan et al. (2013) found holotrichs on tips of outer tentacles of *Aulactinia vancouverensis* Sanamyan et al., 2013, which were hypothesized to be fighting tentacles. In addition, the actiniid *Oulactis concinnata* (Dayton in Dana, 1846) exhibits tentacles that do not possess holotrichs but have searching behavior and are morphologically differentiated from other feeding tentacles (e.g., longer, with different coloration and batteries of large *b*-mastigophores) (Häussermann, 2003). Unlike members of Metridioidea whose fighting tentacles develop from tentacles in inner cycles (often first, or first
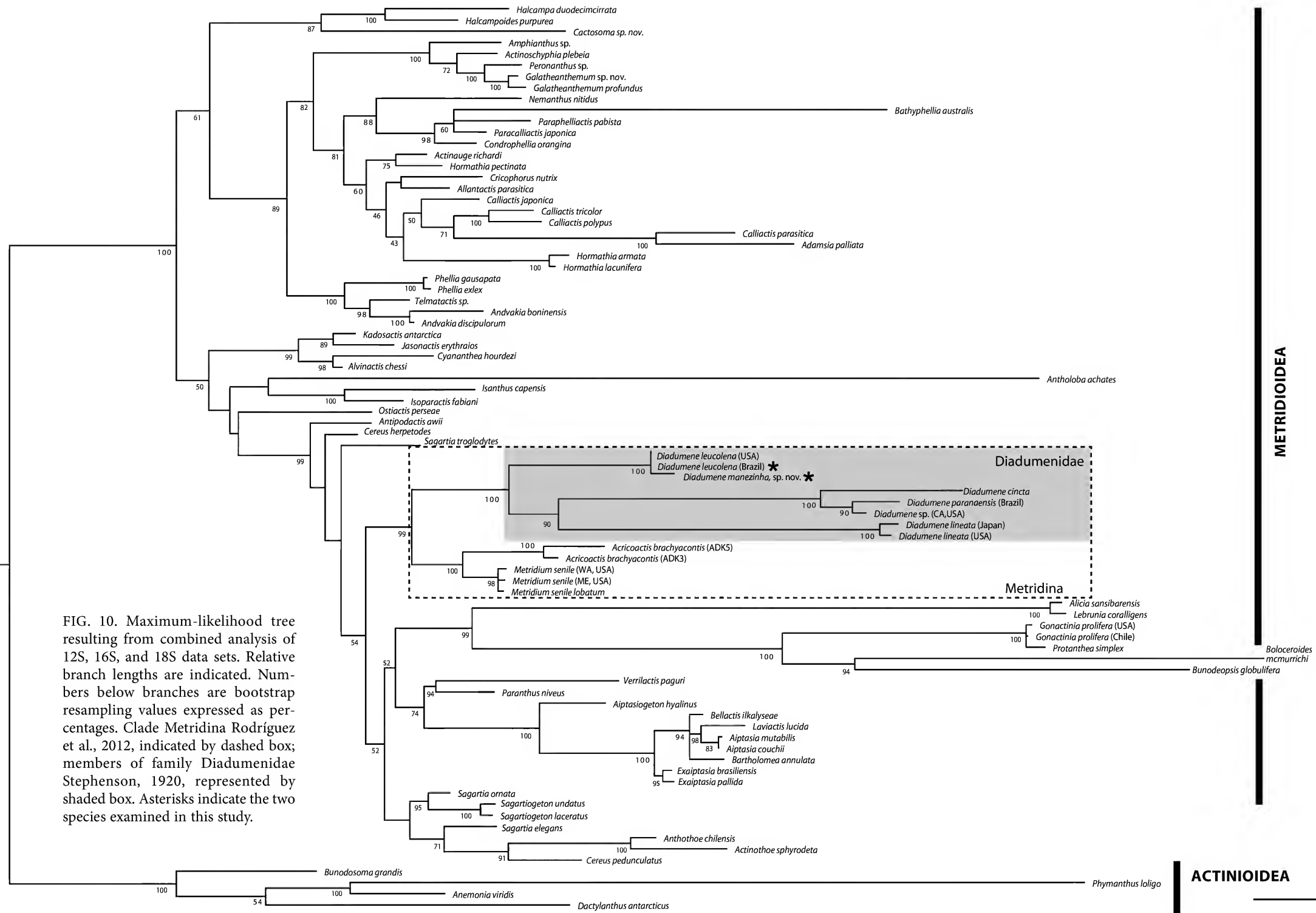
FIG. 10. Maximum-likelihood tree resulting from combined analysis of 12S, 16S, and 18S data sets. Relative branch lengths are indicated. Numbers below branches are bootstrap resampling values expressed as percentages. Clade Metridina Rodríguez et al., 2012, indicated by dashed box; members of family Diadumenidae Stephenson, 1920, represented by shaded box. Asterisks indicate the two species examined in this study.

and second cycles; rarely also third cycle), all fighting tentacles of actinioideans develop from tentacles in outer cycles (Sanamyan et al., 2013). Although fighting tentacles of inner and outer cycles have similar histological and nematocyst content (i.e., holotrichs concentrated on the tip of tentacles: e.g., Williams, 1975; Sanamyan and Sanamyan, 1998), a detailed revision of this structure is necessary to establish homology between fighting tentacles of metridioideans and actinioideans. In addition, whether the tentacles of actiniids are similarly involved in agonistic behavior, as speculated by Häussermann (2003) for those in *O. concinnata*, needs further investigation (Fautin and Chia, 1986).

Nematocysts found in the acontia of *Diadumene leucolena* and *D. manezinha* corresponded to two distinct types that are easily identified from unexploded capsules: basitrichs and *p*-mastigophores B2a. *Diadumene manezinha*, however, has three distinct categories of *p*-mastigophores B2a, a characteristic shared with members of *D. paranaensis*, but whose smallest category does not overlap in size. Carlgren (1924a) recorded three types of nematocysts in the acontia of *D. neozelanica*, which we confirmed from examining syntypes of the species (ZMUC ANT-000076) to be basitrichs and two categories of *p*-mastigophores B2a. Hand (1956) transferred *D. lineata* to a newly erected family (Haliplaneliidae) and genus (*Haliplanella* Hand, 1956) due to a smaller category named microbasic amastigophores found in the acontia of eight populations of the species from California. After Cutress (1955) clarified that microbasic amastigophores also had a terminal tubule and should be regarded as *p*-mastigophores and Williams (1975) found fighting tentacles in populations of *D. lineata* from England and Japan, Manuel (1981) synonymized Haliplanellidae with Diadumenidae, but kept *Haliplanella* as a separate genus. To further distinguish these genera, Manuel (1981) redefined *Diadumene* to include species with only one category of *p*-mastigophores, as the nomenclature used in his study (i.e., Weill, 1934, modified by Carlgren, 1940) did not capture the distinction between the two categories of *p*-mastigophores present in their acontia. Manuel's (1981) diagnosis of *Diadumene* is problematic as it would exclude *D. neozelanica*, *D. paranaensis*, and *D. manezinha* from the genus, contradicting recent phylogenetic analyses (e.g., Grajales and Rodríguez, 2016) and the present study (fig. 10; see Discussion below).

Regardless of its familial or generic placement, the distinction between *Diadumene lineata* and other species became more evident after Pires (1988) described the haliplanelid *Tricnidactis errans* using the cnidae nomenclature of Schmidt (1969, 1972, 1974), which allowed differentiation of *p*-mastigophores in the acontia in two categories: *p*-mastigophores B2a and *p*-mastigophores B1. The presence of these two nematocysts in the acontia has since been confirmed for *T. errans* (Excoffon and Zamponi, 1993) and *D. lineata* (Excoffon et al., 2004; Acuña et al., 2004). The recovered position of *D. lineata* within Diadumenidae in recent phylogenetic analyses (e.g., Rodríguez et al., 2012, 2014; Lauretta et al., 2014; Grajales and Rodríguez, 2016) supports Manuel's (1981) hypothesis that an extra category of *p*-mastigophores did not warrant the erection of the family Haliplanellidae, but does not support the maintenance of *D. lineata* in a separate genus. Thus, the presence of a category of *p*-mastigophores B1 in the acontia of *D. lineata* is interpreted as a specific feature of the species. Given the low frequency of *p*-mastigophores B1 in the acontia of *D. lineata* and *T. errans,* however, it is possible that a

revision of *Diadumene* species will reveal that this feature is more widespread within the genus. Assuming a correct specific identification of their material, many did not find *p*-mastigophores B1 of the smallest category in the acontia of *D. lineata* (Stephenson, 1935; Carlgren, 1945, 1952; Widersten, 1976). Alternatively, a detailed revision of species of *Diadumene* may show that this smaller category of nematocysts in the acontia corresponds instead to *p*-mastigophores B2a as seen in *D. paranaensis* and *D. manezinha*. Given the difficulties involved in the observation of the proximal shaft in small nematocysts (Östman et al., 2010a), distinguishing undischarged capsules of *p*-mastigophores B2a from *p*-mastigophores B1 in acontia of *D. lineata* is difficult and may lead to misclassifications. Observation of undischarged capsules of the small category in acontia of *D. lineata* from Brazil (São Sebastião, São Paulo) suggests that small *p*-mastigophores B1 could be *p*-mastigophores B2 (L.C.G., personal obs.). The fact that tentacles morphologically resembling fighting tentacles have also been observed in members of the family Aiptasiidae Carlgren, 1924a, albeit that confirmation based on cnidae was not possible (E.R., personal obs.), suggests that *T. errans* might belong within Aiptasiidae, a fact that could be supported by other morphological features (e.g., *p*-mastigophores B1 in acontia; presence of a weak mesogleal sphincter at the base of the tentacles).

RELEVANT NOTES ON CNIDAE TERMINOLOGY: Regardless of whether only *Diadumene lineata* or more species of the genus possess *p*-mastigophores B1 in acontia and the reliable identification of nematocysts in this category, the choice of nomenclature used to differentiate *p*-mastigophores may reveal or obscure this feature. The terminology used by Sanamyan et al. (2012) to classify *p*-mastigophores (i.e., Schmidt, 1969, 1972, 1974, modified by den Hartog, 1995) identifies nematocysts without a "Faltstück" (i.e., without a divided shaft) but with bilateral symmetry as *p*-mastigophores B2a. By incorporating the modification of den Hartog (1995), differences between *D. lineata* and other species in the genus as well as among diadumenids and other metridioidean families with "true" *p*-mastigophores B2a with a Faltstück in the acontia gets blurred (e.g., den Hartog and Ates, 2011; Kovtun et al., 2012). For this reason, we chose to use Schmidt's (1969, 1972, 1974) nomenclature to differentiate *p*-mastigophores without the modification of den Hartog (1995) as opposed to Sanamyan et al. (2012); it is worth noticing that the latter authors do not use the terminology "B2c" suggested by den Hartog (1995) to differentiate *p*-mastigophores B1 with bilateral symmetric capsules from *p*-mastigophores B2a *sensu* Schmidt (1969, 1972, 1974). It is especially important to note that den Hartog (1995) corrected what he believed was a mistake made by Schmidt (1969) when he characterized *p*-mastigophores B1 of *Telmatactis* Gravier, 1916, as having a terminal tubule. Den Hartog (1995) differentiates *p*-mastigophores B2c as the only "true" amastigophores unlike *p*-mastigophores B2a of many species within Boloceroididae Carlgren, 1924b, Aiptasiidae, Diadumenidae, and Sagartiidae, which have a vestigial tubule left in the capsule after discharge.

Although we acknowledge that capsules of *p*-mastigophores B1 primarily found in filaments of sea anemones having a distinctive symmetrical ovate or teardrop shape (den Hartog, 1995; Reft, 2012) are different from other nematocyst types as confirmed by Reft (2012), the transfer of bilaterally symmetrical capsules of *p*-mastigophores B1 of andvakiids to category B2 is inconsistent with the more fundamental definition of that category as having a shaft divided in two

parts (i.e., with Faltstück). While this might be interpreted as a semantic conflict, it is important to maintain internal consistency in these already poorly defined categories of cnidae and their conflicting or unparallel terminologies. That symmetry may help distinguish types of nematocysts has been emphasized by Reft (2012) when she created two categories for *p*-mastigophores B2a sensu Schmidt (1969, 1972, 1974) based on symmetrical (*p*-rhabdoids B2s) or asymmetrical capsules (*p*-rhabdoids B2d). Both categories clustered at opposite ends of a continuum with outliers crossing into each other's morphospace (Reft, 2012). Especially *p*-rhabdoids B2d exhibited a broad distribution with no obvious clustering, which suggests this category and its definition may have been misinterpreted (Reft, 2012). The difficulty in correctly assigning nematocysts to this category seen in the discriminant analysis by Reft (2012) further indicates that this category might not be appropriate, with misclassification scattered in several groups with no obvious patterns, including categories *p*-rhabdoids B2s and *p*-rhabdoids B1. Unfortunately, Reft (2012) included only *p*-mastigophores B1 typical of filaments of sea anemones (i.e., ovate/teardrop shaped) from four metridioidean genera in her study, leaving unanswered the question as to whether *p*-mastigophores B1 should be split into subcategories.

Den Hartog (1995) raised an issue regarding the possibility of misclassification of nematocysts due to their immaturity (Reft, 2012). Östman et al. (2010a) interpreted capsules of microbasic amastigophores as immature when they exhibited one or a combination of the following: long and/or broad capsule, long proximal shaft with V-shaped notch closer to the distal capsule may form loops or undulations, and no internal capsular matrix is visible. Likewise, we interpret the *p*-rhabdoids C with undulating shaft found in tentacles of *Diadumene lineata* and *Tricnidactis errans,* and with looped proximal shaft in acontia of *Bellactis ilkalyseae* Dube, 1983, and *Exaiptasia pallida* (Agassiz in Verrill, 1864) recorded by Pinto (2002) as immature *p*-mastigophores B2a. Our hypothesis is supported the larger size range of the supposedly *p*-mastigophores C compared to *p*-mastigophores B2a seen in the same structures. Schmidt (1969, 1972, 1974) differentiated *p*-rhabdoids B2b from *p*-rhabdoids C based on the length of the shaft (i.e., with one and a half longitudinal turns in *p*-rhabdoids B2b and fourfold turns in *p*-rhabdoids C) and the folding of the proximal part of the shaft (i.e., more densely folded due to spine arrangement in *p*-rhabdoids B2b, which explains the similar undischarged shaft length in both types). The nematocysts with undulating or looped shafts classified by Pinto (2002) are not *p*-rhabdoids C under these definitions. In addition, shafts in nematocysts belonging to the medium category of *p*-mastigophores B2a from the acontia of specimens of *D. manezinha* that loop (fig. 11A, B) or undulate (fig. 11C, D) are not rare and often found together with nematocysts with straightened shafts (fig. 11E, F) in squash preparations. These morphologies are interpreted as different developmental stages of *p*-mastigophores B2a as suggested by Östman et al. (2010b) for *p*-mastigophores B2a seen in acontia (Östman et al., 2010b: fig. 6B, C, F) and *p*-mastigophores B2a and *p*-mastigophores B1 in mesenteries (Östman et al., 2010b: fig. 7B–E) of *Metridium senile*. Capsules of *p*-mastigophores B2a with looped, undulating, and straightened shafts have also been observed in other metridioideans (fig. 12). Although we cannot establish a time series for the distinct developmental stages of *p*-mastigophores B2a of *D. leucolena* (fig. 11) and other metridiodeans (fig. 12), we interpret nematocysts with looped (figs.
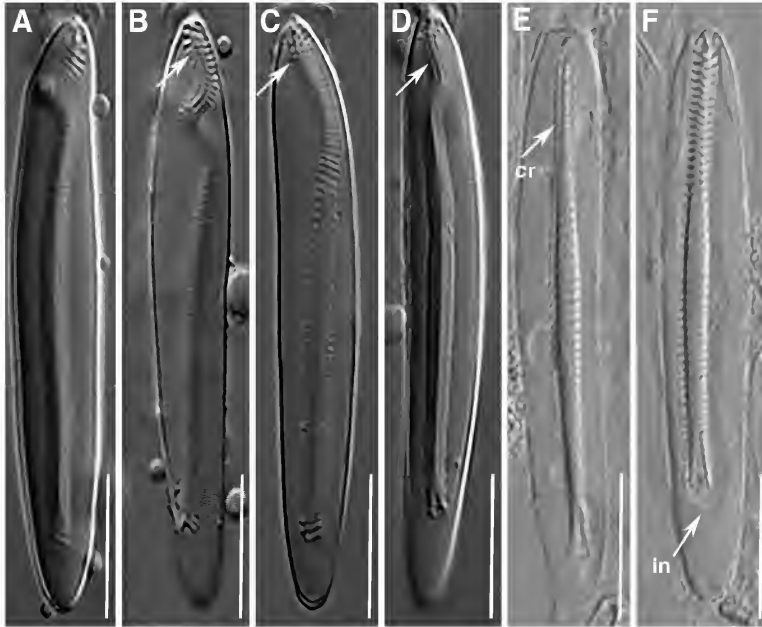
FIG. 11. Differentiation of undischarged medium *p*-mastigophores B2a from acontia of *D. manezinha*, sp. nov. **A,** immature nematocyst with looped proximal part of shaft; **B, C, D,** immature nematocyst with undulating proximal shaft; note increased distance between V-shaped notch of shaft and distal part of capsule, straightening of the shaft, and central rod-shaped structure visible on proximal shaft (arrow); **E,** immature nematocyst with straightened shaft and central rod-shaped structure visible on proximal part of shaft; **F,** nematocyst late in development with limit between proximal and main shaft indistinct, central rod-shaped structure indistinct, and internal capsular matrix visible close to V-shaped notch (note shorter shaft with increased distance between V-shaped notch of shaft and distal part of capsule). Abbreviations: **cr,** central rod-shaped structure; **in,** internal capsular matrix. Scale bars: 10 μm.

11A, 12A, C, H, M, N) or undulating shafts (figs. 11B, C, 12B, D, G, I, J, K, O) as immature stages whose capsules become straighter and whose shaft becomes shorter as the helices tighten (figs. 11E, F, 12E, F, L, P, Q), especially in the proximal region, with a visible central rod-shaped structure on the proximal shaft (figs. 11E, 12E, K, I–K, P) and later without it (figs. 11F, 12F, L, Q) (see Östman et al., 2010b, 2010c).

The two categories of *p*-mastigophores B2a in the acontia of specimens of *Diadumene leucolena* found together in slide preparations of all six specimens examined exhibited a continuous range distribution with overlap in the middle of the range. These two categories may correspond to either two distinct developmental stages of *p*-mastigophores B2 or two distinct size categories of *p*-mastigophores B2a. Mature and immature capsules of *p*-mastigophores B2a found in tentacles of *Metridium senile* were differentiated by Östman et al. (2010a: figs. 1, 2) based on the presence of a rod-shaped structure in immature capsules and the absence of this structure in mature capsules with no clear distinction between the main and proximal parts of the shaft. The categories of *p*-mastigophores B2a found in the acontia of *D. leucolena* may, thus, correspond to immature (fig. 5T) and mature nematocysts (fig. 5S). Additionally, as described by Östman et al. (2010a) for *p*-mastigophores, a shorter basal
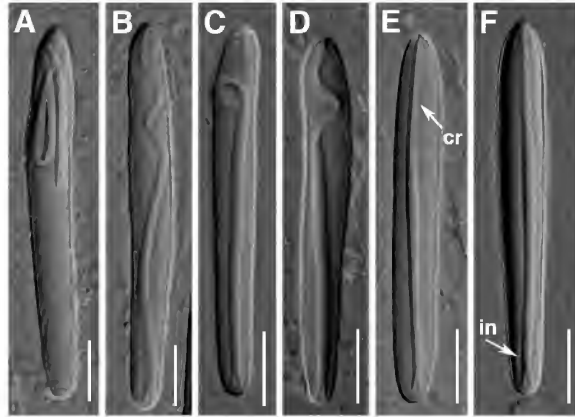
FIG. 12. Undischarged *p*-mastigophores B2a of acontia in different species and various degrees of development. Sagartiidae sp.: **A,** immature nematocyst with broad capsule and looped proximal and main shaft; **B,** immature nematocyst with broad capsule and undulating proximal and main shafts; **C,** immature nematocyst with looped proximal shaft; **D,** immature nematocyst with undulating proximal shaft and distinct limit between proximal and main shaft; **E,** nematocyst late in development showing shorter, straighter proximal and main shaft with visible central rod-shaped rod on proximal shaft; **F,** mature nematocyst with slender capsule and internal capsular matrix visible, straight shaft with indistinct central rod-shaped structure on proximal shaft and indistinct limit between proximal and main shaft. Scale bars: **A–F,** 10 μm.
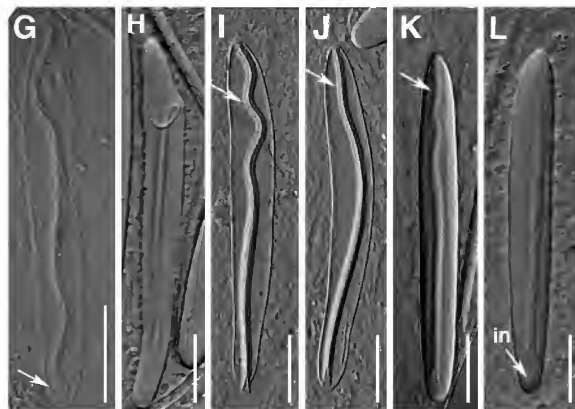

FIG. 12. (*continued*). *Diadumene lineata* (Verrill, 1869a): **G,** immature nematocyst with coiled proximal part of shaft and undulating main shaft with undifferentiated V-shaped notch (arrow); **H,** immature nematocyst with curved capsule and distinct limit between proximal and main shaft forming loop; **I,** immature nematocyst with undulating proximal and main shaft, difference between proximal and main shaft distinct and visible central rod-shaped structure on proximal shaft (arrow); **J,** immature nematocyst with shorter and straighter undulating shaft, difference between proximal and main shaft distinct and central rod-shaped structure visible on proximal shaft (arrow); **K,** nematocyst in late development with straightened main shaft but with visible central rod-shaped structure on proximal shaft (arrow); **L,** fully mature nematocyst with straightened, shorter shaft with internal capsular matrix visible and no distinction between proximal and main shaft. Scale bars: **G,** 20 μm; **H–L,** 10 μm.
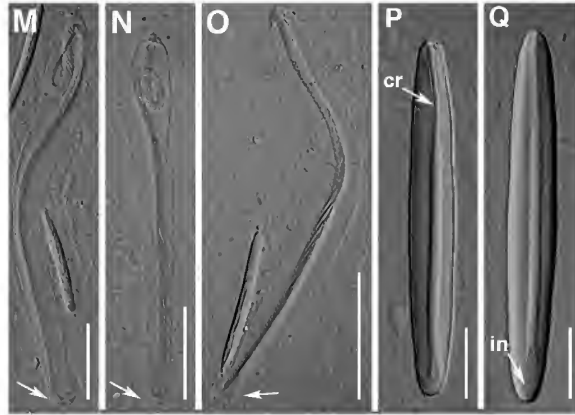
FIG. 12. (*continued*). *Exaiptasia pallida* (Agassiz in Verrill, 1864): **M, N,** immature nematocysts showing looped proximal shaft and undulating main shaft with undifferentiated V-shaped notch (arrow); note the capsule shortening and straightening as it develops; small basitrich seen close to distal part of *p*-mastigophore B2a in M; **O,** immature nematocyst with differentiated V-shaped notch (arrow), straightened proximal shaft distinctly differentiated from main shaft; **P,** nematocyst late in development with distinct limit between proximal and main shaft and distinct central rod-shaped structure; **Q,** mature nematocyst with shorter and straighter shaft, indistinct limit between proximal and main shaft, and visible intracellular capsular matrix. Abbreviations: **cr,** central rod-shaped structure, **in,** internal capsular matrix. Scale bars: **H, M,** 20 μm; **N,** 25 μm; **O,** 30 μm; **P, Q,** 10 μm.

tubule with a corresponding increased distance between the V-shaped notch and the basal capsule wall was observed in presumed mature capsules of *p*-mastigophores B2a (fig. 5S), as opposed to immature ones (fig. 5T) in acontia of *D. leucolena*. Similarly, Carlgren (1924a) found larger, opaque, and curved *p*-mastigophores in the acontia of a large specimen of *D. neozelanica* that he considered a developmental stage of the larger category of *p*-mastigophores. Capsules of *p*-mastigophore B2a recorded in the actinopharynx of *D. leucolena* and *D. manezinha* may correspond to mature (figs. 5L, 9M) and immature ones (figs. 5M, 9N), respectively. For this reason, mature and immature measurements in actinopharynx were combined to give length and width ranges in table 2. That the two categories of *p*-mastigophores B2a recorded in the acontia of *D. paranaensis* are developmental stages of the same type of nematocyst (Beneti et al., 2015: fig. 4Q, S) is also hypothesized here. The fact that presumed immature capsules of *p*-mastigophores B2a seen in acontia of *D. leucolena* are more abundant than mature ones in the examined specimens may be related to the supply and demand of this nematocyst in acontia (Robson, 1988). Even if the two categories of *p*-mastigophores B2a in the acontia of *D. leucolena* are not distinct developmental stages of the same type of nematocyst but rather two distinct types of nematocysts, this character, combined with other anatomical characteristics of the species (e.g., lack of marginal sphincter, holotrichs in tentacles, number and pairs of mesenteries), confirm *D. leucolena*'s classification within Diadumenidae.

DIFFERENTIAL DIAGNOSIS FROM OTHER DIADUMENE SPECIES: Members of *Diadumene* are uniform regarding many anatomical (e.g., presence of cinclides on scapus, six pairs of perfect mesenteries) and microanatomical characters (e.g., all species have retractors diffuse to restricted, parietobasilar and basilar musculature weak), and are distinguished by a mosaic of features related to the column (e.g., distribution of cinclides in column, presence of nematocyst aggregations), mesenteries (e.g., number of cycles, irregularity due to asexual reproduction), cnidae, and geographic distribution. Although the genus *Diadumene* is one of the most diverse within Actiniaria (Carlgren, 1945) in terms of the types of nematocysts, cnidae are at the same time quite uniform across species, making differences potentially informative at the species level (Carlgren, 1940).

The arrangement of cinclides in longitudinal rows seen in the column of *Diadumene leucolena* and *D. manezinha* differentiates them from species with a concentrated band of cinclides on distal scapus (*D. fransciscana*) and those with cinclides scattered throughout the column (*D. schillerianna, D. cincta, D. neozelanica, D. lighti, D. lineata*). Unfortunately, *D. crocata* could not be included in the comparison of *Diadumene* species, given the paucity of information available in the literature on its morphology and cnidae as well as the lack of type material for this species. From the remaining three species with cinclides arranged in longitudinal rows in the column, *D. leucolena* can be differentiated from *D. kameruniensis* by the number of tentacles and mesenteries (91–95 tentacles and up to 5 cycles of mesenteries in *D. leucolena*; up to 192 tentacles and 6 cycles of mesenteries in *D. kameruniensis*) and by the presence of anatomical irregularities due to asexual reproduction in *D. kameruniensis* that are absent in *D. leucolena*. Similarly, *D. leucolena* can be distinguished from *D. neozelanica* by the presence of anatomical irregularities due to asexual reproduction in the latter, as well as by cinclide morphology (cinclides inconspicuous and not on raised projections in *D. neozelanica*; cinclides conspicuous and on top of raised projections in *D. leucolena*), fertility pattern (some mesenteries of the third cycle fertile in *D. neozelanica*; mesenteries of third cycle always sterile in *D. leucolena*), and details of the cnidae (e.g., *p*-mastigophores B1 and large category of *p*-mastigophores B2a present in acontia and *p*-mastigophores A present in actinopharynx of *D. neozelanica* are all absent from *D. leucolena*). In addition to the anatomical irregularities resulting from asexual reproduction seen in *D. paranaensis* and absent in *D. leucolena*, cinclide morphology (cinclides inconspicuous and not on raised projections in *D. paranaensis*; cinclides conspicuous and on top of raised projections in *D. leucolena*), and cnidae details distinguish *D. leucolena* from *D. paranaensis* (e.g., *p*-mastigophores B2a with looped basal tubule in tentacles of *D. paranaensis* are absent from *D. leucolena*; two categories of *non-overlapping p*-mastigophores B2a in acontia of *D. paranaensis* are not found in *D. leucolena*). Specimens of *D. leucolena* examined here closely agree with previous descriptions of the species (e.g., Carlgren, 1950; Hand, 1956), including the Brazilian material identified as *Diadumene* sp. by Pinto (2002). Two categories of *p*-mastigophores B2a in the acontia recorded in all specimens of *D. leucolena* examined in this study have never been described for the species and were not found in the syntypes examined (YPM 665); the cnidae measurements from syntypes closely agree with those given for the Brazilian specimens (table 1), except holotrichs I were not recorded in the

syntypes. We hypothesize that the two categories of *p*-mastigophores B2a are distinct developmental stages of the same type of cnidae (see relevant remarks on cnidae terminology above). Until the relationship between development and morphology of nematocysts is fully understood, we identify the specimens examined in this study as *D. leucolena*, as no other morphological difference exists between these specimens and previous descriptions of the species. This is the first record of *D. leucolena* for the southern hemisphere.

Similarly to *Diadumene leucolena*, *D. manezinha* can be differentiated from *D. kameruniensis* based on the number of mesenteries and tentacles (89–92 tentacles and up to 5 cycles of mesenteries in *D. manezinha*; up to 192 tentacles and 6 cycles of mesenteries in *D. kameruniensis*) and the presence of anatomical irregularities due to asexual reproduction found in *D. kameruniensis* and absent in *D. manezinha*. Unlike *D. manezinha*, whose mesenteries of the third cycle are always sterile and regularly arranged due to absence of asexual reproduction, *D. neozelanica* has some mesenteries of the third cycle fertile and always displays anatomical irregularities due to asexual reproduction. In addition, details of the cnidae, in particular nematocysts in the acontia, clearly differentiate *D. manezinha* and *D. neozelanica*: one category of *p*-mastigophores B2a is found in the acontia of *D. neozelanica* while three categories of *p*-mastigophores B2a are found in *D. manezinha*.

Diadumene manezinha can be easily distinguished from the three species of *Diadumene* recorded from Brazil (i.e., *D. paranaensis*, *D. leucolena*, *D. lineata*). The presence of anatomical irregularities due to asexual reproduction in *D. paranaensis* (absent in *D. manezinha*) and differences in nematocyst content of all tissues (e.g., extra category of *p*-mastigophores B2a in acontia, holotrichs in column, and *p*-mastigophores A in the actinopharynx in *D. manezinha* all absent from *D. paranaensis*; *p*-mastigophores B2b with looped basal tubule in the tentacles of *D. paranaensis* absent from *D. manezinha*) clearly differentiates these two species. Among other features, cinclide morphology (inconspicuous and not on raised projections in *D. manezinhav*; conspicuous and on top of raised projections in *D. leucolena*) and cnidae of acontia differentiate *D. manezinha* from *D. leucolena* (two size categories of *p*-mastigophores B2a in the acontia of *D. leucolena*; three nonoverlapping size categories *p*-mastigophores B2a in *D. manezinha*). *Diadumene manezinha* and *D. lineata* are differentiated by cinclide arrangement in the column (scattered in *D. lineata*; arranged in longitudinal rows in *D. manezinha*), details of cnidae (especially presence of *p*-mastigophores B1 in acontia of *D. lineata*), and anatomical irregularities in number of tentacles and mesenteries in *D. lineata* (often observed in populations of *D. lineata* outside Japan; Stephenson, 1935), which were never observed in *D. manezinha*. Similar to specimens of *D. lineata* from the Black Sea (Kovtun et al., 2012), *D. manezinha* has *p*-mastigophores A in the actinopharynx although they belong to a single category (vs. two categories in *D. lineata*) and are much more slender in *D. manezinha* than in *D. lineata*. Similarly, syntypes of *D. neozelanica* (ZMUC ANT-000076) exhibited *p*-mastigophores A not only in the actinopharynx, but also in the filaments (table 2). In both structures, *p*-mastigophores A of *D. neozelanica* were slender and small, being more similar to those of *D. manezinha* than those of *D. lineata*. *Diadumene manezinha* is the 11th species described for the genus and the fourth *Diadumene* recorded for Brazil.

PHYLOGENETIC ANALYSIS: The phylogenetic relationships and clades recovered in this study agree with earlier broad-scale analyses of sea anemones (e.g., Daly et al., 2008; Gusmão and Daly, 2010; Rodríguez et al., 2012, 2014). The close relationship found between Metridiidae and Diadumenidae has been consistently recovered by most other phylogenetic analyses (e.g., Daly et al., 2008; Gusmão and Daly, 2010; Rodríguez et al., 2012, 2014; Grajales and Rodríguez, 2016; Larson, 2016) and named Clade Metridina by Rodríguez et al. (2012). While this result highlights the morphological similarity between members of Metriididae and Diadumenidae, the placement of Acricoactinidae as sister to Metridiidae in agreement with Larson (2016) presents a new hypothesis for the evolution of the marginal sphincter musculature within this clade. While previous studies predating the description of Acricoactinidae (e.g., Rodríguez et al., 2012, 2014) indicated that this character was lost in Diadumenidae, this new phylogenetic hypothesis suggests that the most parsimonious scenario (at the Metridina clade level) is a single loss of the marginal sphincter muscle, followed by a reappearance in Metridiidae. This would constitute the first instance of a novel evolution of this character within Metridioidea in a similar scenario to the independent evolution of a marginal sphincter in Halcuriidae Carlgren, 1918 (Rodríguez et al., 2014). Another possibility, which has been observed in several lineages within Actiniaria, is the repeated loss of the marginal sphincter muscle in Diadumenidae and Acricoactinidae, a less parsimonious scenario, but consistent with other instances of marginal sphincter loss in correlation to a reduction in size or degeneration and complete loss of acontia (Rodríguez et al., 2014).

The phylogenetic position of the three species of *Diadumene* found in Brazil shows a complex diversification scenario within the genus. While *D. leucolena* and *D. manezinha* exhibit morphological differences consistent with their being two distinct species, they appear as sister taxa in our phylogenetic tree (fig. 10), whereas the close geographical distribution of *D. paranaensis* and *D. manezinha* would suggest that these species would be more closely related. Instead, *D. paranaensis* is nested within a clade composed of species distributed in the northern hemisphere, a result also supported by morphological similarities between *D. paranaensis* and *D. cincta* suggested by Beneti et al. (2015). These two species also share *p*-mastigophores B2 with looped basal tubule in the outer tentacles, a character present in *D. lighti* (Hand, 1956). This author suggested that a new genus within Diadumenidae should be established for species presenting this character, as it differs from the condition found in *D. schilleriana*, the type species of *Diadumene*. A comprehensive revision of the cnidae seen in outer tentacles in other species of the genus as well as their phylogenetic position will be required to make decisive conclusions about the validity of the genus and whether a new genus should be erected.

Currently, molecular data are available for only five of the 11 valid species within the genus, but the inclusion of taxa from other biogeographic regions (e.g., *Diadumene neozelanica, D. schilleriana*) will undoubtedly contribute to our understanding of the diversification process within the group. Under the current scenario, it is clear that at least two nonrelated lineages of *Diadumene* are present in the southern hemisphere. Finally, the presence of *D. leucolena* in Brazil further confirms that some species within the genus have extensive distribution ranges, as it is the case of *D. lineata*, long considered a cosmopolitan species (Minasian, 1982; Podbiel-

ski et al., 2016). Due to the variability and the limited sampling within each species, conclusions about how these species disperse (e.g., natural process vs. human intervention) are beyond the scope of this study.

UTILITY OF MICROCOMPUTED CT SCANNING FOR THE TAXONOMY OF ACTINIARIA: In this study we evaluate the utility of micro-CT imaging for the taxonomy and systematics of sea anemones, which has been possible only as a result of recent protocol modifications of contrast enhancement in soft-bodied invertebrates (e.g., Metscher, 2009a, 2009b; Faulwetter et al., 2013a, 2013b; Descamps et al., 2014; Paterson et al., 2014; Fernández et al., 2014; Tessler et al., 2016; Holst et al., 2016). The appeal of micro-CT scanning for sea anemone studies is its potential to facilitate and improve characterization of morphological characters used in the taxonomy of the group especially in regard to the tridimensional anatomical representations based on of micro-CT images. Currently, morphological studies in Actiniaria combine complementary techniques: gross dissections provide information on internal features in three dimensions with low resolution whereas histology provides resolution at the cellular level in two dimensions. Hence, micro-CT methods combine qualities of both methods (i.e., high resolution with tridimensional qualities) with comparable cost (Chandler and Volz, 2004) while avoiding some of their shortcomings (e.g., slowness, sample preparation, small volumes, artifacts) (Shearer et al., 2016). When compared to dissections and histology, micro-CT scanning is also presumed to be nondestructive, easy, and fast. Thus, sea anemone taxonomy would highly benefit from incorporation of micro-CT data given the paucity of morphological characters whose number remain essentially unchanged since the beginning of modern studies (i.e., Hertwig, 1882, sensu Danielssen, 1890) and the difficulties involved in the establishment of primary homologies in the group. This often obscures our understanding of evolutionary patterns and morphological convergence found in molecular phylogenetic studies (e.g., Gusmão and Daly, 2010; Rodríguez et al., 2012, 2014). Hence, methods that can provide insights into details of traditionally used characters are imperative to advance our understanding of sea anemone systematics and evolution.

The protocol employed in this study (adapted from Tessler et al., 2016) using osmium tetroxide involved successfully staining the material so external and internal features were readily recognized in micro-CT scans (figs. 4, 8) as well as in resulting 3D renderings (figs. 4, 8). Staining is a crucial stage of micro-CT studies and is directly related to the final resolution of images of other soft-bodied organisms successfully stained with osmium tetroxide as a contrast enhancer (Handschuh et al., 2013; Fernández et al., 2014; Holst et al., 2016; Tessler et al., 2016), including other soft-bodied cnidarians (i.e., staurozoans, Holst et al., 2016). The core of *Diadumene manezinha* (fig. 8B, E, F), however, showed imperfect staining, which is probably a result of the self-limiting properties of osmium tetroxide due to large size and thickness of this specimen. This means that osmium tetroxide may not be be able to penetrate the tissues of large species of sea anemones, such as deep-sea ones, or it may penetrate too slowly to be practical. Likewise, phosphotungstic acid (PTA), known to stain muscle tissues more intensely (Metscher, 2009a), also presents depth limitations with a diffusion rate of approximately 1 mm per week (Fernández et al., 2014). Although PTA is far less toxic and simpler to use and dispose of compared with osmium tetroxide, it works best with alcohol-fixed specimens, rarely the case

for freshly collected sea anemones, which are usually fixed in formalin for histological purposes. Perhaps for this reason, staining of sea anemones fixed in formalin and stained with 0.3% PTA in 70% ethanol did not lead to improvement in the resolution of details of the musculature in the material examined even when staining was successful (results not shown; L.C.G., personal obs.). Although iodine has been efficiently used to stain a variety of soft tissues (Metscher, 2009a, 2009b), the penetration of iodine was unsatisfactory during tests (results not shown; A.G., personal obs.), resulting in images with poor contrast and low resolution. We recommend the use of osmium tetroxide for chemical staining of sea anemones, but emphasize that differences in size, thickness, consistency, and texture of different species may require adaptation of the protocol used in this study depending on their physical properties.

The high-contrast micro-CT images obtained (figs. 4, 8) ensured that all relevant external and internal anatomical features of sea anemones were satisfactorily characterized. Micro-CT images were confirmed in observation of whole specimens and the traditionally used dissections and histology. These characters included hard-to-observe traits such as columnar cinclides (fig. 4A–E), small mesenteries without retractors (figs. 4F, G, 8E–G), basilar musculature (figs. 4L, 8J) and fertility patterns (fig. 8F), all of which are critical for correct identification of certain genera and species of actiniarians. Unprecedented for sea anemone taxonomy, reliable representation of the scanned specimens in 3D reconstructions was remarkable and corroborated the findings seen in the 2D micro-CT scans, but was particularly important in the establishment of mesentery growth patterns (figs. 4I, 8G) and comparison of the number of mesenteries proximally and distally (figs. 4G–I, 8E–G). This was a result of the ability to observe characters without having to section whole specimens, which is extremely laborious and time-consuming to the point of being impractical using histology (Shearer et al., 2016); high-contrast micro-CT offered us the possibility of examining a specimen from multiple angles that does not have to be fixed a priori, as is the case for histology (Dinley et al., 2010; Berquist et al., 2012), and of manipulating a region of interest to depict a single character without obscuring others, something difficult to achieve in practice in dissections (Faulwetter et al., 2013a; Fernández et al., 2014; Tessler et al., 2016). Accuracy in the definition of these characters (e.g., growth patterns are used to distinguish *Phelliactis* Simon, 1892, and *Paraphelliactis* Carlgren, 1928; fertility patterns are important in defining *Chondrophellia* Carlgren, 1925, *Amphianthus* Hertwig, 1882, *Stephanauge* Verrill, 1899) and whether they contain any phylogenetic signal can be evaluated only when their presence and variability is accurately determined.

A limitation of the incorporation of micro-CT in taxonomic studies of sea anemones, however, pertains to determination of microanatomical musculature details: although it is possible to discern retractor (figs. 4G–H, J, 8E–F) and basilar musculature (figs. 4L, 8J) and their general morphology, the resolution obtained in the images did not permit observation of musculature details. Although microdetails in musculature are not used to distinguish *Diadumene* species, this shows that application of micro-CT may not be appropriate to study groups in which these microanatomical features (especially of musculature) are necessary for proper taxonomic descriptions. Micro-CT scanning may not be appropriate to study taxa for which the number of muscle processes in retractor or parietal musculature (e.g., Edwardsiidae de

Quatrefages, 1842), observation of small sphincter musculature (e.g., Aiptasiidae or Haliplanellidae), or tentacle musculature (e.g., Actinostolidae Carlgren, 1893) are relevant. In addition, although tissue layers (i.e., epidermis, mesoglea and gastrodermis) exhibited varying attenuation levels in *D. leucolena* (fig. 4B–F) and *D. manezinha* (fig. 8B–D), tentacle musculature was not visible in scans of either species (figs. 4F, 8D). One drawback of micro-CT is that small marginal sphincter musculature cannot be determined from the scans (L.C.G. and A.G., personal obs.), as the resolution achieved in our studies was far coarser compared to that of histological sections, but this musculature can be observed in species that possess large mesogleal or endodermal marginal sphincters (results not shown). For the present study, the distinction is moot, since members of *Diadumene* do not possess marginal sphincter musculature. Given technical properties of the scanner, resolution is a trade-off between size and scanning time with higher resolution achieved faster in smaller specimens (Paterson et al., 2014). The muscle fibers of retractors, parietal or marginal sphincter musculature, for example, are probably at the resolution limit of the micro-CT scanner and cannot be portrayed with an appropriate resolution for proper observation. We agree with Holst et al. (2016) in that resolving issues of species complexes and cryptic species is not currently possible using micro-CT scanning and 3D renderings due to the method's low resolution compared with traditional techniques. Focusing on a small region of interest by dissecting the specimen can potentially increase image resolution up to the technical limit of the scanner, but tridimensional information is lost in the process.

The micro-CT scanning of the two species of *Diadumene* shows that this imaging technique can be a valuable tool to characterize taxonomic characters and maximize the potential of anatomical studies in Actiniaria. It is also possible that a different set of technical characteristics of the scanner (e.g., larger scanner detector) might improve the final resolution of the images in order to overcome the limitations observed for microanatomy. The speed with which 2D micro-CT images were acquired (i.e., on the order of hours) is a clear advantage of this method over histology, which can take several days and require specialized equipment and training (Shearer et al., 2016). This is only partly true, as manipulation of rendered images to display and isolate specific features was very time-consuming. Although micro-CT scanning speeds up the stage of obtaining data, unless the access to a micro-CT is unlimited (which was not the case for this study), the number of specimens scanned (i.e., low; one specimen in this study) prevents detection of variability and differences at the species level. Similarly, the non-destructive nature of micro-CT scanning is often proclaimed as a clear advantage of this method over dissections, and particularly over histology (Metscher, 2009a, 2009b; Dinley et al., 2010; Paterson et al., 2014; Nesteruk and Wiśniewski, 2015;). In our case, however, osmium tetroxide irreversibly changes tissue characteristics (Faulwetter et al., 2013a) and cannot be washed off after scanning (Fernández et al., 2014), rendering the specimens unusable for any other purpose. The high toxicity of osmium tetroxide makes its use as a staining agent a clear problem for valuable material.

The use of micro-CT would be especially advantageous when studying anemones that exhibit highly modified morphologies, which present a challenge for histology (e.g., members of *Adamsia*

Forbes, 1840, *Amphianthus*, *Peronanthus* Hiles, 1899, *Monactis* (Gravier, 1918)). In cases in which micro-CT may not provide sufficient resolution, the combination of this technique with traditional ones (i.e., histology) is advisable. For sea anemones, this might be particularly important given that the microanatomical data on tissue derivation, shape, and development of musculature as well as reproductive structures and details of other structures provided by histology are essential for the identification to the species level (Spano and Flores, 2013). In addition, the necessity of squash preparations and examination of unstained samples (which provides size ranges and distribution of cnidae in a specimen) prevents the complete replacement of standard techniques by micro-CT alone. For this reason, virtual cybertypes (see Faulwetter et al., 2013a; Akkari et al., 2015) may never be appropriate for Actiniaria, but we agree with others (e.g., Faulwetter et al., 2013a; Fernández et al., 2014) that virtual representation can be a viable way to transfer data as well as being a potential tool for teaching (Berquist et al., 2012). Finally, given differences in size, consistency, texture, and thickness seen in different groups of sea anemones, the protocol provided in this study should be modified to the requirements and properties of each group. If combined with techniques tradition- ally used in sea anemone taxonomic studies, micro-CT scanning has the potential to solve morpho- logical ambiguity, especially regarding characters for which tridimensionality is highly beneficial, thus helping resolve existing taxonomic issues in Actiniaria.

ACKNOWLEDGMENTS

REFERENCES

Acuña, F.H., L. Ricci, A.C. Excoffon, and M.O. Zamponi. 2004. A novel statistical analysis of cnidocysts in acontiarian sea anemones (Cnidaria, Actiniaria) using generalized linear models with gamma errors. Zoologischer Anzeiger 243: 47–52.

Akkari, N., H. Enghoff, and B.D. Metscher. 2015. A new dimension in documenting new species: high-detail imaging for myriapod taxonomy and first 3D cybertype of a new millipede species (Diplopoda, Julida, Julidae). PLoS ONE 10: e0135243.

Andres, A. 1884. Le Attinie (Monografia). Leipzig, Germany: Verlag von Wilhelm Engelmann.

Belém, M.J.C., and D.C. Monteiro. 1977. Contribuições ao conhecimento da fauna de cnidários do Rio de Janeiro. II. *Haliplanella luciae* (Verrill, 1988) (Actinaria, Acontiaria), uma nova ocorrência no Brasil. Avulsos do Museu Nacional 26: 1–19.

Beneti, J.S., S.N. Stampar, M.M. Maronna, A.C. Morandini, and F.L. Silveira. 2015. A new species of *Diadumene* (Actiniaria: Diadumenidae) from the subtropical coast of Brazil. Zootaxa 4021 (1): 156–168.

Berquist, R.M., et al. 2012. The Digital Fish Library: using MRI to digitize, database, and document the morphological diversity of fish. PLoS ONE 7: e34499.

Carlgren, O. 1893. Studien über nordische Actinien. Kungliga Svenska Vetenskapsakademiens Handlingar 25: 1–148.

Carlgren, O. 1918. Die Mesenterienanordnung der Halcuriiden. Kungliga Fysiografiska Sällskapets Handlingar 29: 1–37.

Carlgren, O. 1924a. Actiniaria from New Zealand and its subantarctic islands (papers from Dr. Th. Mortensen's Pacific Expedition 1914–16. XXI). Videnskabelige Meddelelser fra Dansk Naturhistorisk Forening (Copenhagen) 77: 179–261.

Carlgren, O. 1924b. On *Boloceroides*, *Bunodeopsis* and their supposed allied genera. Arkiv für Zoologi 17A: 1–20.

Carlgren, O. 1925. Zur Kenntnis der Hexacorallen. Zoologischer Anzeiger 65, 87–99.

Carlgren, O. 1927. Actiniaria. *In* Th. Monod (editor), Faune des colonies françaises. Contribution á l'étude de la faune du Cameroun: 475–480. Paris: Société d'Éditions Géographiques, Maritimes et Coloniales.

Carlgren, O. 1928. Ceriantharier, Zoantharier och Actiniarier. Meddelelser om Grønland 23: 253–308.

Carlgren, O. 1929. Über eine Actiniariengattung mit besonderen Fangtentakeln. Zoologischer Anzeiger 81: 109–113.

Carlgren, O. 1934. Zur Revision der Actiniaren. Arkiv för Zoologi 18: 1–36.

Carlgren, O. 1940. A contribution to the knowledge of the structure and distribution of the cnidae in the Anthozoa. Kungliga Fysiografiska Sällskapets Handlingar 51: 1–62.

Carlgren, O. 1945. Further contributions to the knowledge of the cnidom in the Anthozoa especially in the Actiniaria. Kungliga Fysiografiska Sällskapets Handlingar 56: 1–24.

Carlgren, O. 1949. A survey of Ptychodactiaria, Corallimorpharia and Actiniaria. Kungliga Svenska Vetenskapsakademiens Handlingar 1: 1–121.

Carlgren, O. 1950. A revision of some Actiniaria described by A.E. Verrill. Journal of the Washington Academy of Sciences 40: 22–28.

Carlgren, O. 1952. Actiniaria from North America. Arkiv für Zoologi 3 (20): 373–390.

Chandler, G.T., and D.C. Volz. 2004. Semiquantitative confocal laser scanning microscopy applied to marine invertebrate ecotoxicology. Marine Biotechnology 6: 128–137.

Cutress, C.E. 1955. An interpretation of the structure and distribution of Cnidae in Anthozoa. Systematic Zoology 4: 120–137.

Cutress, C.E. 1961. *Habrosanthus bathamae*, n. gen., n. sp. (Actiniaria: Sagartiidae) from New Zealand. Transactions of the Royal Society of New Zealand 1 (6): 95–101.

Daly, M., A. Chaudhuri, L.C. Gusmão, and E. Rodríguez. 2008. Phylogenetic relationships among sea anemones (Cnidaria: Anthozoa: Actiniaria). Molecular Phylogenetics and Evolution 48: 292–301.

Dalyell, J. G. 1848. Rare and remarkable animals of Scotland. London: John Van Voorst.

Dana, J. D. 1846. Zoophythes. *In* United States Exploring Expedition during years 1838, 1840, 1841, 1842 under the command of Charles Wilkes, U.S.N. Philadelphia: Lea and Blanchard.

Danielssen, D.C. 1890. *Actinida*. Den Norske Nordhavs-Expedition 1876–1878. Zoologi. Christiania, Denmark: Grøndahl & Søn.

Descamps, E., et al. 2014. Soft tissue discrimination with contrast agents using micro-CT scanning. Belgian Journal of Zoology 144: 20–40.

Dinley, J., et al. 2010. Micro-computed X-ray tomography: a new non-destructive method of assessing sectional, fly-through and 3D imaging of a soft-bodied marine worm. Journal of Microscopy 238: 123–133.

Dube, V.M.C. 1983. Contribution to the study of the sea-anemones from the state of Bahia-Brazil - Part V - *Bellactis ilkalysea* gen. nov. sp. nov. Natura 83 (5): 82–193.

Edmands, S., and D.G. Fautin. 1991. Redescription of *Aulactinia veratra* n. comb. (= *Cnidopus veratra*) (Coelenterata: Actiniaria) from Australia. Records of the Western Australian Museum (Perth) 15: 59–68.

Excoffon, A.C., and M.O. Zamponi. 1993. Anemonas de Mar del Plata y localidades vecinas. IV. *Tricnidactis errans* Pires, 1988 (Actiniaria, Haliplanellidae). Iheringia 75: 47–53.

Excoffon, A.C., F.H. Acuña, and M.O. Zamponi. 2004. Presence of *Haliplanella lineata* (Verrill, 1869) (Actiniaria, Haliplanellidae) in the Argentine Sea and the finding of anisorhize haploneme cnidocyst. Physis 60: 1–6.

Farrapeira, C.M. 2010. Shallow water Cirripedia of the northeastern coast of Brazil: the impact of life history and invasion on biogeography. Journal of Experimental Marine Biology and Ecology 392 (1): 210–219.

Farrapeira, C.M., A.V. Melo, D.F. Barbosa, and K.M. Silva. 2007. Ship hull fouling in the Port of Recife, Pernambuco. Brazilian Journal of Oceanography 55 (3): 207–221.

Faulwetter, S., A. Vasileiadou, M. Kouratoras, D. Thanos, and C. Arvanitidis. 2013a. Micro-computed tomography: introducing new dimensions to taxonomy. Zookeys 263: 1–45.

Faulwetter, S.T., T. Dailianis, A. Vasileiadou, and C. Arvanitidis. 2013b. Contrast enhancing techniques for the application of micro-CT in marine biodiversity studies. Microscopy and Analysis 27 (2): S4–S7.

Fautin, D.G. 1988. The importance of nematocysts to actiniarian taxonomy. *In* D.A. Hessinger and H.M. Lenhoff (editors), The biology of nematocysts: 487–500. New York: Academic Press.

Fautin, D.G. 2013. Hexacorallians of the World. Internet resource (http://hercules.kgs.ku.edu/hexacoral/anemone2/index.cfm), accessed January 30, 2018.

Fautin, D.G., and F. Chia. 1986. Revision of sea anemone genus *Epiactis* (Coelenterata: Actiniaria) on the Pacific coast of North America, with descriptions of two new brooding species. Canadian Journal of Zoology 64: 1665–1674.

Fernández, R., S. Kvist, J. Lenihan, G. Giribet, and A. Ziegler, A. 2014. *Sine systemate chaos*? A versatile tool for earthworm taxonomy: non-destructive imaging of freshly fixed and museum specimens using micro-computed tomography. PLoS ONE 9 (5): e96617.

Forbes, E. 1840. On the British Actiniadae. Annual Magazine of Natural History 5: 180–184.

Fukui, Y. 1986. Catch tentacles in the sea anemone *Haliplanella luciae*: role as organs of social behavior. Marine Biology 91: 245–251.

Gollasch, S., and K. Riemann-Zürneck. 1996. Transoceanic dispersal of benthic macrofauna: *Haliplanella luciae* (Verrill, 1898) (Anthozoa, Actiniaria) found on a ship's hull in a shipyard dock in Hamburg Harbour, Germany. Helgoländer Meeresuntersuchungen 50 (2): 253–258.

Gosse, P.H. 1858. Synopsis of the families, genera, and species of the British Actiniae. Annals and Magazine of Natural History 1: 414–419.

Grajales, A., and E. Rodríguez. 2016. Elucidating the evolutionary relationships of the Aiptasiidae, a widespread cnidarian–dinoflagellate model system (Cnidaria: Anthozoa: Actiniaria: Metridioidea). Molecular Phylogenetics and Evolution 94: 252–263.

Gravier, C. 1916. Sur un type nouveau d'actinie de l'île San Thomé (Golfe de Guinée). Bulletin du Muséum National d'Histoire Naturelle (Paris) 22 (5): 234–236.

Gravier, C. 1918. Note préliminaire sur les hexactiniaires recueillis au cours des croisières de la Princesse-Alice et de l'Hirondelle de 1888 a 1913 inclusivement. Bulletin de l'Institut Océanographique (Monaco) 34: 1–24.

Gusmão, L.C., and Daly, M. 2010. Evolution of sea anemones (Cnidaria: Actiniaria: Hormathiidae) symbiotic with hermit crabs. Molecular Phylogenetics and Evolution 56: 868–877.

Hand, C. 1956. The sea anemones of central California Part III. The acontiarian anemones. Wasmann Journal of Biology 13: 189–251.

Hand, C. 1957. Another sea anemone from California and the types of certain Californian anemones. Journal of the Washington Academy of Sciences 47: 411–414.

Hand, C. 1961. Two new acontiate New Zealand sea anemones. Transactions of the Royal Society of New Zealand 1 (4): 75–89.

Handschuh, S., N. Baeumler, T. Schwaha, and B. Ruthensteiner. 2013. A correlative approach for combining microCT, light and transmission electron microscopy in a single 3D scenario. Frontiers in Zoology 10: 44.

Hartog, J.C. den. 1995. The genus *Telmatactis* Gravier, 1916 (Actiniaria: Isophellidae) in Greece and the eastern Mediterranean. Zoologische Mededelingen 69: 53–176.

Hartog, J.C. den, and R.M. Ates. 2011. Actiniaria from Ria de Arosa, Galicia, northwestern Spain, in the Netherlands Centre for Biodiversity Naturalis, Leiden. Zoologische Mededelingen 85: 11–53.

Häussermann, V. 2003. Redescription of *Oulactis concinnata* (Drayton in Dana, 1846) (Cnidaria: Anthozoa: Actiniidae), an actiniid sea anemone from Chile and Perú with special fighting tentacles; with a preliminary revision of the genera with a "frond-like" marginal ruff. Zoologische Verhandelingen 345: 173–209.

Hertwig, R. 1882. Die Actinien der Challenger Expedition. Jena, Germany: Gustav Fischer.

Hiles, I.L. 1899. The Gorgonacea collected by Dr. Willey. *In* Arthur Willey, Zoological results based on material from New Britain, New Guinea, Loyalty Islands and elsewhere, vol. 2: 195–206.

Holst, S., P. Michalik, M. Noske, J. Krieger, and I. Sötje. 2016. Potential of X-ray micro-computed tomography for soft-bodied and gelatinous cnidarians with special emphasis on scyphozoan and cubozoan statoliths. Journal of Plankton Research 38 (5): 1225–1242.

Hutton, F.W. 1880. Contributions to the coelenterate fauna of New Zealand. Transactions and Proceedings of the New Zealand Institute 12: 274–276.

Johnston, G. 1847. A history of British Zoophytes. London: John Van Voorst.

Katoh, K., K. Misawa, K.I. Kuma, and T. Miyata. 2002. MAFFT: a novel method for rapid multiple sequence alignment based on fast Fourier transform. Nucleic Acids Research 30 (14): 3059–3066.

Kearse, M., et al. 2012. Geneious Basic: an integrated and extendable desktop software platform for the organization and analysis of sequence data. Bioinformatics 28 (12): 1647–1649.

Kovtun, O. A., N.P. Sanamyan, and A.V. Martynov. 2012. Invasive anemone *Diadumene lineata* (Anthozoa: Actiniaria: Diadumenidae) in northern part of the Black. Морський екологічний журнал (Morskoï ĕkologicheskiĭ zhurnal) 4: 27–38.

Kruszynski, K. J., R. van Liere, and J.A. Kaandorp. 2006. An interactive visualization system for quantifying coral structures. Proceedings Eurographics/IEEE VGTC Symposium on Visualization: 283–290.

Kwietniewski, C.R. 1898. Actiniaria von Ambon und Thursday Island. *In* Zoologische Forschungreisen in Australien und dem malayischen Archipel von Richard Semon. Vol. 5, Systematik, Tiergeographie, Anatomie wirbelloser Tiere: 385–430. Jena: Gustav Fischer.

Lanfear, R., B. Calcott, S.Y. Ho, and S. Guindon. 2012. PartitionFinder: combined selection of partitioning schemes and substitution models for phylogenetic analyses. Molecular biology and evolution 29 (6): 1695–701.

Larson, P. 2016. *Acricoactis brachyacontis* sp. nov. from Adak Island, Alaska, represents a new genus and family of metridioidean sea anemone (Anthozoa: Hexacorallia: Actiniaria). Marine Biodiversity. [doi: 10.1007/s12526-016-0582-2]

Larson, P., and M. Daly. 2015. 'Putting names with faces': a description of *Epiactis handi* sp. nov. helps to solve taxonomic confusion in species of the sea anemone *Epiactis* (Actiniaria, Actiniidae). Journal of Marine Biological Association of the United Kingdom 16.

Lauretta, D., V. Häussermann, M.R. Brugler, and E. Rodríguez, E. 2014. *Isoparactis fionae* sp. n. (Cnidaria: Anthozoa: Actiniaria) from southern Patagonia with a discussion of the family Isanthidae. Organisms Diversity & Evolution 14 (1): 31–42.

Linnaeus, C. 1761. Fauna Svecica. Stockholm: Laurentii Salvii.

Manuel, R.L. 1981. British Anthozoa keys and notes for the identification of the species. London: Academic Press.

McMurrich, J.P. 1887. Notes on the fauna of Beaufort, North Carolina. Studies at the Biological Laboratory of the Johns Hopkins University 4: 55–63.

Metscher, B.D. 2009a. MicroCT for comparative morphology: simple staining methods allow high-contrast 3D imaging of diverse non-mineralized animal tissues. BMC Physiology 9: 11.

Metscher, B.D. 2009b. MicroCT for developmental biology: a versatile tool for high-contrast 3D imaging at histological resolutions. Developmental Dynamics 238: 632–640.

Miller, M.A., W. Pfeiffer, and T. Schwartz. 2010. Creating the CIPRES Science Gateway for inference of large phylogenetic trees. Proceedings of the Gateway Computing Environments Workshop (GCE): 1–8.

Minasian, L.L. 1982. The relationship of size and biomass to fission rate in a clone of the sea anemone, *Haliplanella luciae* (Verrill). Journal of Experimental Marine Biology and Ecology 58 (2): 151–62.

Molina, L.M., M.S. Valiñas, P.D. Pratolongo, R. Elias, and G.M. Perillo. 2009. First record of the sea anemone *Diadumene lineata* (Verrill, 1871) associated to *Spartina alterniflora* roots and stems, in marshes at the Bahia Blanca estuary, Argentina. Biological Invasions 11 (2): 409–16.

Morales Pinzón, A.M., et al. 2014. A semi-automatic method to extract canal pathways in 3D micro-CT images of octocorals. PLoS ONE 9 (1): e85557.

Nesteruk, T., and L. Wiśniewski. 2015. Microtomography in morphological studies of small invertebrates. Teka Komisji Ochrony i Kształtowania Środowiska Przyrodniczego O.L. PAN 12: 62–70.

Östman, C., J.R. Kultima, and C. Roat. 2010a. Tentacle cnidae of the sea anemone *Metridium senile* (Linnaeus, 1761) (Cnidaria: Anthozoa). Scientia Marina 74 (3): 511–521.

Östman, C., J.R. Kultima, C. Roat, and K. Rundblom. 2010b. Acontia and mesentery nematocysts of the sea anemone *Metridium senile* (Linnaeus, 1761) (Cnidaria: Anthozoa). Scientia Marina 74 (3): 483–497.

Östman, C., J.R. Kultima, and S.Y.G. Wong. 2010c. Dart formation in nematocysts of the sea anemone Metridium senile (Linnaeus, 1761) (Cnidaria: Anthozoa). Scientia Marina 74 (3): 499–510.

Paterson, G.L.J., et al. 2014. The pros and cons of using micro-computed tomography in gross and micro-anatomical assessments of polychaetous annelids. Memoirs of Museum Victoria 71: 237–246.

Pennant, T. 1777. A British zoology. Vol. 4. London: Benj. White.

Pinto, S.M. 2002. Anêmonas-do-mar com acôncios (Anthozoa: Actiniaria: Mesomyaria): análises morfológica e molecular. Master's thesis, University of São Paulo, São Paulo.

Pires, D.O. 1988. *Tricnidactis errans*, n. gen., n. sp., (Cnidaria, Actiniaria, Haliplanellidae) from Guanabara Bay, Rio de Janeiro, Brazil. Revista Brasileira de Biologia 48 (3): 507–516.

Podbielski, I., C. Bock, M. Lenz, and F. Melzner. 2016. Using the critical Salinity (Scrit) concept to predict invasion potential of the anemone *Diadumene lineata* in the Baltic Sea. Marine Biology 163: 227.

Presnell, J.K., and M.P. Schreibman. 1997. Humason's animal tissue techniques. Baltimore, MD: Johns Hopkins University Press.

Puce, S., et al. 2011. Three-dimensional analysis of the canal network of an Indonesian *Stylaster* (Cnidaria, Hydrozoa, Stylasteridae) by means of X-ray computed microtomography. Zoomorphology 130: 85–95.

Purcell, J.E. 1977. Aggressive function and induced development of catch tentacles in the sea anemone *Metridium senile* (Coelenterata, Actiniaria). Biological Bulletin 153: 355–368.

Purcell, J.E., and C.L. Kitting. 1982. Intraspecific aggression and population distributions of the sea anemone *Metridium senile*. Biological Bulletin 162: 345–349.

de Quatrefages, A. (1842). Mémoire sur les Edwardsies (*Edwardsia*, nob.) nouveau genre de la famille des Actinies. Annales des Sciences Naturelles 18: 65–109

Rafinesque, C.S. 1815. Analyse de la nature ou Tableau de l'univers et des corps organisés. Palermo, Italy: C. S. Rafinesque.

Reft, A.J. 2012. Understanding the morphology and distribution of nematocysts in sea anemones and their relatives. Ph.D. dissertation, Ohio State University, Columbus.

Riemann-Zürneck, K. 1975. Actiniaria des Südwestatlantik II. Sagartiidae and Metridiidae. Helgoländer wissenschaflichen Meeresuntersuchungen 27: 70–95.

Robson, A.E. 1988. Problems of supply and demand for cnidae in Anthozoa. *In* D.A. Hessinger and H.M. Lenhoff (editors), The biology of nematocysts: 179–207. San Diego: Academic Press.

Rocha, R., et al. 2013. The need of more rigorous assessments of marine species introductions: a counter example from the Brazilian coast. Marine Pollution Bulletin 67: 241–243.

Roche, R.C., R.A. Abel, K.G. Johnson, and C.T. Perry. 2010. Quantification of porosity in *Acropora pulchra* (Brook, 1891) using X-ray micro-computed tomography techniques. Journal of Experimental Marine Biology and Ecology 396 (1): 1–9.

Rodríguez, E., and M. Daly. 2010. Phylogenetic relationships among deep-sea and chemosynthetic sea anemones: Actinoscyphiidae and Actinostolidae (Actiniaria: Mesomyaria). PLoS One 5 (6): e1095.

Rodríguez, E., M. Barbeitos, M. Daly, L.C. Gusmão, and V. Häussermann. 2012. Toward a natural classification: phylogeny of acontiate sea anemones (Cnidaria, Anthozoa, Actiniaria). Cladistics 28 (4): 375–92.

Rodríguez, E., et al. 2014. Hidden among sea anemones: the first comprehensive phylogenetic reconstruction of the order Actiniaria (Cnidaria, Anthozoa, Hexacorallia) reveals a novel group of hexacorals. PLoS ONE 9 (5): e96998.

Sanamyan, N.P., and K.E. Sanamyan. 1998. Some Actiniaria from the Commander Islands (Cnidaria: Anthozoa). Zoosystematica Rossica 7 (1): 1–8.

Sanamyan, N.P., K.E. Sanamyan, and K.R. Tabachnick. 2012. The first species of Actiniaria, *Spongiactis japonica* gen. n., sp. n. (Cnidaria: Anthozoa), an obligate symbiont of a glass sponge. Invertebrate Zoology 9: 127–141.

Sanamyan, N.P., K.E. Sanamyan, and N. McDaniel. 2013. Two new shallow water sea anemones of the family Actiniidae (Cnidaria: Anthozoa: Actiniaria) from British Columbia (NE Pacific). Invertebrate Zoology 10: 199–216.

Schmidt, H. 1969. Die Nesselkapseln der Aktinien und ihre differentialdiagnostische Bedeutung. Helgoländer Wissenschaftliche Meeresuntersuchungen 19: 284–317.

Schmidt, H. 1972. Die Nesselkapseln der Anthozoen und ihre Bedeutung fur die phylogenetische Systematik. Helgoländer Wissenschaftliche Meeresuntersuchungen 23: 422–458.

Schmidt, H. 1974. On evolution in the Anthozoa. Proceedings of the Second International Coral Reef Symposium 1: 533–560.

Sentoku, A., et al. 2015. Regular budding modes in a zooxanthellate dendrophylliid *Turbinaria peltata* (Scleractinia) revealed by X-ray CT imaging and three-dimensional reconstruction. Journal of Morphology 276: 1100–1108.

Shearer, T., R.S. Bradley, A. Hidalgo-Bastida, M.J. Sherratt, and S.H. Cartmell. 2016. Three-dimensional visualization of soft biological structures by X-ray computed micro-tomography. Journal of Cell Science 129: 2483–2492.

Shick, J.M., and A.N. Lamb. 1977. Asexual reproduction and genetic population structure in the colonizing sea anemone *Haliplanella luciae*. Biological Bulletin 153 (3): 604–617.

Da Silveira, F.L., and A.C. Morandini. 2011. Checklist dos Cnidaria do Estado de São Paulo, Brasil. Biota Neotropica 11 (1a): 1–11.

Simon, J.A. 1892. Ein Beitrag zur Anatomie und Systematik der Hexactinien. München, Germany: Val. Hvfling.

Spano, C., and V. Flores. 2013. Staining protocol for the histological study of sea anemones (Anthozoa: Actiniaria) with recommendations for anesthesia and fixation of specimens. Latin American Journal of Aquatic Research 41: 1019–1024.

Stamatakis, A. 2006. RAxML-VI-HPC: maximum likelihood-based phylogenetic analyses with thousands of taxa and mixed models. Bioinformatics 22 (21): 2688–2690.

Stephenson, T.A. 1920. On the classification of Actiniaria. Part I. Forms with acontia and forms with a mesogloeal sphincter. Quarterly Journal of Microscopical Science 64: 425–574.

Stephenson, T.A. 1925. On a new British sea anemones. Journal of the Marine Biological Association of the United Kingdom 13: 880–890.

Stephenson, T.A. 1935. The British sea anemones. Vol. 2. London: Ray Society.

Stoliczka, F. 1869. On the anatomy of *Sagartia schilleriana* and *Membranipora bengalensis*, a new coral and bryozoon living in brackish water at Port Canning. Journal of the Asiatic Society of Bengal 38: 28–63.

Tessler, M., A. Barrio, E. Borda, R. Rood-Goldman, M. Hill, and M.E. Siddall. 2016. Description of a soft-bodied invertebrate with microcomputed tomography and revision of the genus *Chtonobdella* (Hirudinea: Haemadipsidae). Zoologica Scripta 45: 552–565.

Torrey, H.B. 1902. Papers from the Harriman Alaska expedition. XXX. Anemones, with a discussion of variation in *Metridium*. Proceedings of the Washington Academy of Sciences 4: 373–410.

Uchida, T. 1932. Occurrence in Japan of *Diadumene luciae*, a remarkable actinian of rapid dispersal. Journal of the faculty if science, Hokkaido Imperial University 2 (2): 69–82.

Verrill, A.E. 1864. Revision of the Polypi of the eastern coast of the United States. Memoirs of the Boston Society of Natural History 1: 1–45.

Verrill, A.E. 1866. On the polyps and echinoderms of New England, with descriptions of new species. Proceedings of the Boston Society of Natural History 10: 333–357.

Verrill, A.E. 1868. Our sea-anemones. American Naturalist 5: 251–262.

Verrill, A.E. 1869a. Synopsis of the polyps and corals of the North Pacific exploring, under commodore C. Ringgold and Capt. John Rodgers, U.S.N., from 1853 to 1856. Collected by Dr. Wm. Stimpson, naturalist to the expedition. Part IV. Actiniaria. Proceedings of the Essex Institute 6: 51–104.

Verrill, A.E. 1869b. Review of the corals and polyps of the West Coast of America. Transactions of the Connecticut Academy of Arts and Sciences 1: 377–567.

Verrill, A.E. 1898. Descriptions of new American actinians, with critical notes on other species, I. American Journal of Science and Arts 6: 493–498.

Verrill, A.E. 1899. Descriptions of imperfectly known and new actinians, with critical notes or other species, III. American Journal of Science and Arts 7: 143–146.

Verrill, A.E., S.I. Smith, and O. Hager. 1873. Catalogue of the marine invertebrate animals of the southern coast of New England, and adjacent waters. *In* U.S. Commission of Fish and Fisheries (editor), Report on the condition of the sea fisheries of the south coast of New England in 1871 and 1872 (pt. 1): 537–741.

Watson, G.M., and R.N. Mariscal. 1983a. Comparative ultrastructure of catch tentacles and feeding tentacles in the sea anemone *Haliplanella*. Tissue & Cell 15 (6): 939–953.

Watson, G.M., and R.N. Mariscal. 1983b. The development of a sea anemone tentacle specialized for aggression: morphogenesis and regression of the catch tentacle of *Haliplanella luciae* (Cnidaria, Anthozoa). Biological Bulletin 164: 506–517.

Weill, R. 1934. Contribution a l'étude des cnidaires et de leurs nématocystes. Paris, France: Les Presses Universitaires de France.

Widersten, B. 1976. Ceriantharia, Zoanthidae, Corallimorpharia, and Actiniaria from the continental shelf and slope off the eastern coast of the United States. Fishery Bulletin 74 (4): 857–878.

Williams, R.B. 1975. Catch-tentacles in sea anemones: Occurrence in *Haliplanella luciae* (Verrill) and a review of current knowledge. Journal of Natural History 9: 241–248.

Zabin, C.J., J.T. Carlton, and L.S. Godwin. 2004. First report of the Asian sea anemone *Diadumene lineata* from the Hawaiian Islands. Bishop Museum Occasional Papers 79: 54–58.

Zamponi, M.O., M.J.C. Belém, E. Schlenz, and F.H. Acuña. 1998. Distribution and some ecological aspects of Corallimorpharia and Actiniaria from shallow waters of the South American Atlantic Coasts. Physis: 31–45.